14. Eliopoulos N, Al-Khaldi A, Crosato M, Lachapelle K, Galipeau J. A neovascularized organoid derived from retrovirally engineered bone marrow stroma leads to prolonged in vivo systemic delivery of erythropoietin in nonmyeloablated, immunocompetent mice. Gene Ther. 2003;10(6):478–89.
15. Itaka K, Kataoka K. Progress and prospects of polyplex nanomicelles for plasmid DNA delivery. Curr Gene Ther. 2011;11 (6):457–65.
16. Kanayama N, Fukushima S, Nishiyama N, Itaka K, Jang WD, Miyata K, et al. A PEG-based biocompatible block catiomer with high buffering capacity for the construction of polyplex micelles showing efficient gene transfer toward primary cells. ChemMedChem. 2006;1(4):439–44.
17. Itaka K, Ohba S, Miyata K, Kawaguchi H, Nakamura K, Takato T, et al. Bone regeneration by regulated in vivo gene transfer using biocompatible polyplex nanomicelles. Mol Ther. 2007;15(9):1655–62.
18. Masago K, Itaka K, Nishiyama N, Chung UI, Kataoka K. Gene delivery with biocompatible cationic polymer: pharmacogenomic analysis on cell bioactivity. Biomaterials. 2007;28(34):5169–75.
19. Harada-Shiba M, Takamisawa I, Miyata K, Ishii T, Nishiyama N, Itaka K, et al. Intratracheal gene transfer of adrenomedullin using polyplex nanomicelles attenuates monocrotaline-induced pulmonary hypertension in rats. Mol Ther. 2009;17(7):1180–6.
20. Itaka K, Kataoka K. Recent development of nonviral gene delivery systems with virus-like structures and mechanisms. Eur J Pharm Biopharm. 2009;71(3):475–83.
21. Miyata K, Oba M, Nakanishi M, Fukushima S, Yamasaki Y, Koyama H, et al. Polyplexes from poly(aspartamide) bearing 1,2-diaminoethane side chains induce pH-selective, endosomal membrane destabilization with amplified transfection and negligible cytotoxicity. J Am Chem Soc. 2008;130(48):16287–94.
22. Miyata K, Nishiyama N, Kataoka K. Rational design of smart supramolecular assemblies for gene delivery: chemical challenges in the creation of artificial viruses. Chem Soc Rev. 2012;41(7):2562–74.
23. Itaka K, Ishii T, Hasegawa Y, Kataoka K. Biodegradable polyamino acid-based polycations as safe and effective gene carrier minimizing cumulative toxicity. Biomaterials. 2010;31(13):3707–14.
24. Uchida S, Itaka K, Chen Q, Osada K, Ishii T, Shibata MA, Harada-Shiba M, Kataoka K. PEGylated polyplex with optimized PEG shielding enhances gene introduction in lungs by minimizing inflammatory responses. Mol Ther. 2012;20(6):1196–203
25. Chen Q, Osada K, Ishii T, Oba M, Uchida S, Tockary TA, et al. Homo-catiomer integration into PEGylated polyplex micelle from block-catiomer for systemic anti-angiogenic gene therapy for fibrotic pancreatic tumors. Biomaterials. 2012;33(18):4722–30.
26. Howard RB, Christensen AK, Gibbs FA, Pesch LA. The enzymatic preparation of isolated intact parenchymal cells from rat liver. J Cell Biol. 1967;35(3):675–84.
27. Berry MN, Friend DS. High-yield preparation of isolated rat liver parenchymal cells: a biochemical and fine structural study. J Cell Biol. 1969;43(3):506–20.
28. Tateno C, Yoshizato K. Long-term cultivation of adult rat hepatocytes that undergo multiple cell divisions and express normal parenchymal phenotypes. Am J Pathol. 1996;148(2):383–92.
29. Wurdinger T, Badr C, Pike L, de Kleine R, Weissleder R, Breakefield XO, et al. A secreted luciferase for ex vivo monitoring of in vivo processes. Nat Meth. 2008;5(2):171–3.
30. Nahmias Y, Berthiaume F, Yarmush ML. Integration of technologies for hepatic tissue engineering. Adv Biochem Eng Biotechnol. 2007;103:309–29.
31. Hafez IM, Maurer N, Cullis PR. On the mechanism whereby cationic lipids promote intracellular delivery of polynucleic acids. Gene Ther. 2001;8(15):1188–96.
32. Lv H, Zhang S, Wang B, Cui S, Yan J. Toxicity of cationic lipids and cationic polymers in gene delivery. J Control Release. 2006;114(1):100–9.
33. Han M, Oba M, Nishiyama N, Kano MR, Kizaka-Kondoh S, Kataoka K. Enhanced percolation and gene expression in tumor hypoxia by PEGylated polyplex micelles. Mol Ther. 2009;17 (8):1404–10.
34. Bhatia SN, Yarmush ML, Toner M. Controlling cell interactions by micropatterning in co-cultures: hepatocytes and 3T3 fibroblasts. J Biomed Mater Res. 1997;34(2):189–99.
35. Nishida K, Yamato M, Hayashida Y, Watanabe K, Yamamoto K, Adachi E, et al. Corneal reconstruction with tissue-engineered cell sheets composed of autologous oral mucosal epithelium. N Engl J Med. 2004;351(12):1187–96.
36. Ohashi K, Yokoyama T, Yamato M, Kuge H, Kanehiro H, Tsutsumi M, et al. Engineering functional two- and three-dimensional liver systems in vivo using hepatic tissue sheets. Nat Med. 2007;13(7):880–5.
37. Sekine H, Shimizu T, Dobashi I, Matsuura K, Hagiwara N, Takahashi M, et al. Cardiac cell sheet transplantation improves damaged heart function via superior cell survival in comparison with dissociated cell injection. Tissue Eng Part A. 2011;17(23–24):2973–80.

Journal of Controlled Release 160 (2012) 542–551

Contents lists available at SciVerse ScienceDirect

Journal of Controlled Release

journal homepage: www.elsevier.com/locate/jconrel

Effective transgene expression without toxicity by intraperitoneal administration of PEG-detachable polyplex micelles in mice with peritoneal dissemination

Michiaki Kumagai [a], Shinya Shimoda [a], Rie Wakabayashi [a], Yumi Kunisawa [a], Takehiko Ishii [b], Kensuke Osada [c], Keiji Itaka [d], Nobuhiro Nishiyama [d], Kazunori Kataoka [c], Kenji Nakano [a,*]

[a] Innovation Center for Medical Redox Navigation, Kyushu University, 3-1-1 Maidashi, Higashi-ku, Fukuoka, Fukuoka 812-8582 Japan
[b] Department of Bio Engineering, Graduate School of Engineering, The University of Tokyo, 7-3-1 Hongo, Bunkyo-ku, Tokyo 113-0033, Japan
[c] Department of Materials Engineering, Graduate School of Engineering, The University of Tokyo, 7-3-1 Hongo, Bunkyo-ku, Tokyo 113-0033, Japan
[d] Division of Clinical Biotechnology, Center for Disease Biology and Integrative Medicine, Graduate School of Medicine, The University of Tokyo, 7-3-1 Hongo, Bunkyo-ku, Tokyo 113-0033, Japan

ARTICLE INFO

Article history:
Received 11 November 2011
Accepted 23 March 2012
Available online 30 March 2012

Keywords:
Polyplex micelle
Disulfide linkage
Gene delivery
Peritoneal dissemination
Intraperitoneal administration

ABSTRACT

Block copolymer of poly(ethylene glycol)-*block*-poly{N-[N-(2-aminoethyl)-2-aminoethyl]aspartamide} (PEG-P[Asp(DET)]) has been originally introduced as a promising gene carrier by forming a nanomicelle with plasmid DNA. In this study, the polyplex micelle of PEG-SS-P[Asp(DET)], which disulfide linkage (SS) between PEG and cationic polymer can detach the surrounding PEG chains upon intracellular reduction, was firstly evaluated with respect to *in vivo* transduction efficiency and toxicity in comparison to that of PEG-P[Asp(DET)] in peritoneally disseminated cancer model. Intraperitoneal (i.p.) administration of PEG-SS-P[Asp(DET)] polyplex micelles showed a higher ($P<0.05$) transgene expression compared with PEG-P[Asp(DET)] in tumors. In contrast, the delivered distribution of the micelles was not different between the two polyplex micelles. PEG-SS-P[Asp(DET)] micelle encapsulating human tumor necrosis factor α (hTNF-α) gene exhibits a higher antitumor efficacy against disseminated cancer compared with PEG-P[Asp(DET)] or saline control. No hepatic and renal toxicities were observed by the administration of polyplex micelles. In conclusion, PEG-detachable polyplex micelles may represent an advantage in gene transduction *in vivo* over PEG-undetachable polyplex micelles after i.p. administration for peritoneal dissemination of cancer.

1. Introduction

Gene therapy has attracted much attention as a promising modality to treat intractable diseases, such as genetic disorder, neurodegenerating disease and cancer [1,2]. Viral vectors, such as adenovirus vector, have been vigorously explored in these strategies, because the gene transfer efficiency is generally higher than nonviral gene vector. However, the clinical use of viral vectors has considerable limitations with respect to safety, and it is desirable to develop a nonviral vector. Recently, PEG-based cationic polymers (catiomers) have been expected as one of promising alternatives to viral gene vectors [3–8]. The block catiomers spontaneously associate with plasmid DNA (pDNA) to form sub-100 nm polyplex micelles with high colloidal stability by hydrophilic PEG palisade surrounding the core under physiological conditions and substantial transfection activity [9–14].

We have demonstrated that polyplex micelles formed by PEG-*block*-poly(aspartamide) copolymers carrying the *N*-(2-aminoethyl)-2-aminoethyl group in the side chain (PEG-P[Asp(DET)]) exhibit high efficiency and low cytotoxicity [15]. The polyplex micelles demonstrated appreciable gene transfer into vascular lesions in animal model [16] and bone defect in animal models [17]. To further achieve successful *in vivo* gene therapy, we have tried to modify the block copolymer, because P[Asp(DET)] homopolymer polyplexes show higher transfection efficiency than PEG-P[Asp(DET)] micelles [18] and the PEG palisade surrounding P[Asp(DET)] cores hampers the gene transfection (PEG dilemma) [19–21]. To overcome the dilemma, we have developed PEG detachable polyplex micelles with disulfide linkages between PEG and P[Asp(DET)], which are sensitive to the intracellular reducing environment [22]. This micelle showed higher gene transfection efficiency than the micelle without disulfide linkages by several orders of magnitude *in vitro* assay [22]. However, the transduction on efficacy and safety for *in vivo* application remains to be evaluated.

Systemic chemotherapy is mainly conducted for the patients bearing refractory advanced malignancies, such as liver or lung metastasis and peritoneal dissemination [23,24]. Among these metastases, peritoneal lesions exhibit relative resistance to systemic chemotherapy due to peritoneal-plasma barrier, which prevents the effective drug delivery from blood vessels into the peritoneal lesions

* Corresponding author. Tel.: +81 92 642 6209; fax: +81 92 642 6024.
E-mail address: kenakano@med.kyushu-u.ac.jp (K. Nakano).

0168-3659/$ – see front matter © 2012 Elsevier B.V. All rights reserved.
doi:10.1016/j.jconrel.2012.03.021

[25]. In comparison with conventional systemic chemotherapy, the intraperitoneal (i.p.) administration of hydrophobic chemotherapeutic agents or vectors encapsulated therapeutic genes appears to have an advantage for peritoneal dissemination, because the drugs are directly delivered into the peritoneal cavity and retarded in tumor nodules, which enables to keep high dose concentration in tumor tissues [26]. In addition, gene therapy prevents the rapid enzymatic degradation of therapeutic molecules, such as tumor necrosis factor α (TNF-α), which is known to exhibit anti-tumor effect for a wide variety of cancers [27], and the inflammation-related toxicity induced by its systemic administration of high dose cytokines, although tumor vasculature-specific ligands could increase an accumulation of RGD4C-TNF-α into tumor vicinities [28,29].

In this study, we examined the feasibility of PEG detachable polyplex micelles on transduction efficiency, therapeutic efficacy and safety as a gene delivery system compared with the conventional polyplex without disulfide linkage. The intraperitoneal administration of PEG-detachable polyplex micelles with RGD4C-TNF-α-encoding plasmid, but not that of PEG-undetachable polyplex, revealed an appreciable *in vivo* gene expression and antitumor effect against peritoneal metastases of pancreatic cancer, despite of no difference in the preferable distribution for tumor and lymphatic tissues.

2. Materials and methods

2.1. Chemicals

α-Methoxy-ω-hydroxyl PEG (PEG-OH, $M_n = 12{,}000$, $M_w/M_n = 1.03$) β-benzyl L-aspartate *N*-carboxyanhydride (BLA-NCA) were obtained from NOF Corporation (Tokyo, Japan) and Chuo Kaseihin Co., Inc. (Tokyo, Japan). Methanol (MeOH), 2-aminoethanethiol, diethyl ether, ammonia (NH_3), hexane, ethyl acetate (AcOEt), and hydrochloric acid (HCl) were purchased from Wako Pure Chemical Industries, Ltd. (Osaka, Japan) and used as received. Dichloromethane (CH_2Cl_2), *N*,*N*-dimethylformamide (DMF), diethylenetriamine (DET) and *N*-methyl-2-pyrrolidone (NMP) were purchased from Tokyo Chemical Industry Co. Ltd. (Tokyo, Japan) or Nacalai Tesque (Kyoto, Japan) and purified by distillation before use. Linear polyethyleneimine (LPEI, $M_w = 22{,}000$) was purchased from Polysciences, Inc. (Warrington, PA). Water was purified using a Milli-Q instrument (Millipore, Bedford, MA).

2.2. Synthesis and characterization of PEG-SS-P[Asp(DET)]

PEG-SS-P[Asp(DET)] was prepared as previously reported [22] with minor modification. Briefly, PEG-OH was converted to PEG-SH [30], of which conversion rate was estimated as 80% from ^{1}H NMR spectrum. The crude PEG-SH (0.85 g) was dissolved in MeOH (30 mL), followed by the reaction with 2-aminoethanethiol (100 equiv, 0.65 g) at room temperature to obtain PEG-SS-NH_2. The polymer components were precipitated into an excess amount of diethyl ether, and then the filtrate was dried *in vacuo*. PEG-SS-NH_2 was isolated from the crude product by passing through an ion-exchange gel (SP Sephadex C-50, GE Healthcare, Tokyo, Japan) column. Adsorbed PEG-SS-NH_2 was eluted from the gel by diluted NH_3 aqueous solution, evaporated using rotary evaporator at 30 °C, and then lyophilized as a white powder (0.63 g in yield). The functionality of the PEG end to the aminoethanethiol moiety was confirmed to be 97% by an ion-exchange HPLC equipped with TSKgel SP-5PW column (TOSOH Corporation, Tokyo, Japan).

The PEG-SS-poly(β-benzyl L-aspartate) (PEG-SS-PBLA) block copolymer was prepared by the ring opening polymerization of BLA-NCA (3.3 mmol, 0.97 g) in CH_2Cl_2/DMF (10/1 (v/v), 23 mL) at 35 °C from the terminal primary amino group of PEG-SS-NH_2 (0.04 mmol, 0.50 g). The reaction mixture was added into an excess amount of hexane/AcOEt (6/4 (v/v)), and then the filtrate was dried *in vacuo* (1.17 g in yield). The degree of polymerization (DP) of PBLA was calculated to be 69 by ^{1}H NMR spectroscopy based on the peak intensity of benzyl protons of PBLA ($-OCH_2C_6H_5$, δ = 7.3 ppm) to the ethylene protons in PEG ($-OCH_2CH_2$, δ = 3.6 ppm).

Lyophilized PEG-SS-PBLA (230 mg) was dissolved in NMP (9 mL), followed by the reaction with DET (4 mL, 50 equiv to benzyl group of PBLA segment), diluted in NMP (4 mL) under anhydrous conditions at 5 °C. After 30 min, the reaction mixture was slowly added dropwise into a 5 N HCl aqueous solution, where the temperature of the mixture was kept below 5 °C. Then the mixture was dialyzed against 0.01 N HCl and, subsequently, deionized water (MWCO: 12–14 kDa) at 4 °C. The final solution was lyophilized to obtain PEG-SS-P[Asp(DET)] (Fig. 1) as the chloride salt form (213 mg in yield). The quantitative substitution from BLA to Asp(DET) was confirmed by the peak disappearance of benzyl protons ($-OCH_2C_6H_5$, δ = 7.3 ppm) and the intensity ratio of the ethylene protons in the 1,2-diaminoethani moiety ($H_2N(CH_2)_2NH(CH_2)_2NH$-, δ = 3.4–2.8 ppm) to the methylene protons in PEG ($-OCH_2CH_2$, δ = 3.6 ppm) in the ^{1}H NMR spectrum in D_2O (data not shown).

2.3. Plasmid DNA construction

A plasmid encoding luciferase (pCpG-ΔLuc) was kindly supplied from Dr. Makiya Nishikawa (Kyoto University) [31]. As expression plasmids encoding therapeutic gene, pVIVO-RGD4C-hTNF-α and pCpG-RGD4C-hTNF-α were constructed as follows; the oligonucleotide encoding RGD4C (CDCRGDCFC) with glycine–serine linker interposed between RGD4C and matured human TNF-α (hTNF-α) sequences as a spacer was synthesized. The open-read frame of RGD4C-hTNF-α was integrated at the multi-cloning sites in the plasmid DNA of pVIVO1-mcs with hamster 78-kDa glucose-regulated protein (GRP78) promoter which yields persistent high expression within the tumor micro-environment or in the plasmid of pCpGfree-mcs to delete immunogenic CpG motifs with human elongation factor 1 alpha core promoter (Invivogen, San Diego, CA). The plasmid DNA was amplified in competent DH5R *Escherichia coli* and purified using EndoFree Plasmid Giga Kits (QIAGEN Inc., Valencia, CA). The pDNA concentration was determined by reading the absorbance at 260 nm.

2.4. Preparation of PEG-SS-P[Asp(DET)]/pDNA polyplex micelles

The PEG-SS-P[Asp(DET)] block copolymer and pDNA were separately dissolved in 10 mM Tris–HCl buffer (pH 7.4). The polymer solution was added to a 2-times-excess volume of 375 μg/mL pDNA solution (final pDNA concentration: 250 μg/mL) at N/P ratio = 10, which is a molar ratio of amine units in block cationers to phosphate units in pDNA. The mixed solution was left at 4 °C for 15 min to form polyplex micelles and then subjected to the following experiments. Just prior to *in vivo* administration, 1/10 volume of 1.5 M NaCl solution was added to form isotonic solution. The polyplexes with PEG-P[Asp(DET)] block copolymer (*M*w of PEG: 12,000; DP of P[Asp(DET)] segment: 65) or LPEI were similarly prepared and used as controls.

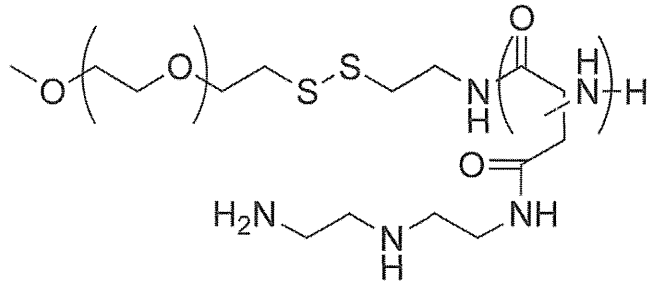

Fig. 1. Chemical structure of PEG-SS-PAsp(DET).

2.5. Dynamic light scattering (DLS) and ζ-potential measurements

DLS and ζ-potential measurements were carried out at 25 °C using an ELSZ-SV2 (Otsuka Electronics Co., Ltd., Osaka, Japan), equipped with a He–Ne ion laser (633 nm) as the incident beam. The polyplex solutions were prepared at 250 μg pDNA/mL in 10 mM Tris–HCl buffer (pH 7.4) at N/P ratio = 10. In the DLS mesurement, the light scattering data were obtained with a detection angle of 160° at 25 °C. The rate of decay in the photon correlation function was analyzed by the cumulant method, and the corresponding hydrodynamic diameter of the polyplexes was then calculated by the Stokes–Einstein equation. In the case of ζ-potential measurement, the ζ-potential was calculated from the obtained electrophoretic mobility by the Smoluchowski equation:

$$\zeta = 4\pi\eta\upsilon/\varepsilon$$

where η is the viscosity of the solvent, υ is the electrophoretic mobility, and ε is the dielectric constant of the solvent.

2.6. Cell lines

Human pancreatic carcinoma SUIT-2 was obtained from the American Type Culture Collection. SUIT-2 stably expressing luciferase protein (SUIT-2/luc) was established by cloning with limiting dilution method after transfecting a multiply attenuated lenti viral vector for luciferase gene provided by Dr. Takafumi Nakamura (The University of Tokyo). SUIT-2 and SUIT-2/luc cells were grown in RPMI1640 (Wako Pure Chemical Industries, Ltd.) supplemented with 10% heat-inactivated fetal bovine serum (FBS, Wako Pure Chemical Industries, Ltd.), 100 U/mL penicillin and 100 μg/mL streptomycin at 37 °C in humidified air containing 5% CO_2.

2.7. Animals

BALB/c nude and BALB/c mice (female, 6 weeks old) were purchased from Charles River Laboratories (Tokyo, Japan). Animals were housed in a temperature-controlled room under 12:12 h light:dark cycles and allowed to access food and water *ad libitum*. Experiments were carried out in compliance with the Guidelines for Animal Experiments of the Kyushu University, and approved by the Animal Care and Use Committee of Kyushu University.

2.8. Kinetic assay for transgene expression by in vivo bioluminescent imaging

BALB/c nude mice were intraperitoneally inoculated with SUIT-2 cells (1×10^6 cells/mouse). One week later, polyplex micelles consisting of 100 μg of pCpG-ΔLuc and block copolymers were administered intraperitoneally. *In vivo* bioluminescent imaging (BLI) was performed with an IVIS Imaging System (Xenogen Biosciences, Alameda, CA) and the bioluminescent signals were analyzed using Living Image software (Xenogen Biosciences, Alameda, CA). At 20 min prior to *in vivo* imaging, animals received the substrate D-Luciferin (Summit Pharmaceuticals International Corporation, Tokyo, Japan) at 75 mg/kg in 10 mM phosphate buffered solution (pH = 7.4) by intraperitoneal injection under anesthesia with the inhalation of 3% isoflurane (Abbot Laboratories, North Chicago, IL).

2.9. Antitumor activity of RGD4C-hTNF-α gene therapy for peritoneal dissemination

BALB/c nude mice (female, n = 10 in each group) were intraperitoneally inoculated with SUIT-2/luc cells (2×10^5 cells/mouse). Tumors were allowed to grow for 1 week. Subsequently, polyplex micelles of PEG-SS-P[Asp(DET)] or PEG-P[Asp(DET)] (50 μg of pVIVO-RGD4C-hTNF-α; N/P ratio = 10) or saline were administered into the peritoneal cavity of mice. We used pVIVO-RGD4C-hTNF-α for cancer therapy experiments, because the GRP promoter of pVIVO1 yields persistently higher expression within the tumor microenvironments than elongation factor-1 promoter of pCpGfree mcs plasmid. In a separate experiment, we confirmed the antitumor efficacy of RGD4C-hTNF-α by comparing pCpG-RGD4C-hTNF-α and mock (pCpGfree-mcs) plasmids to delete immunogenic CpG motifs in peritoneal dissemination model (Supplementary Fig. 1). *In vivo* bioluminescent imaging (BLI) was performed with an IVIS Imaging System as described above (Section 2.8). The survival of the mice was evaluated in each group up to 120 days after the inoculation.

2.10. Analysis of RGD4C-hTNF-α expression by quantitative real-time reverse-transcriptional PCR (qRT-PCR)

The expression of RGD4C-hTNF-α mRNA in tumor and normal organ tissues was evaluated by qRT-PCR. At 24 h after the injection of polyplex micelles, tumor and the other organ tissues (spleen, liver, kidney, lung and intestine) were obtained and snap-frozen in liquid nitrogen for the following assays. Total RNA was extracted using illustra™ RNAspin Mini RNA Isolation Kit (GE Healthcare UK, Ltd., Buckinghamshire, UK) according to the manufacturer's instruction, and subjected to cDNA synthesis using Transcriptor First Strand cDNA synthesis Kit (Roche Applied Science, Mannheim, Germany). Quantitative real-time PCR for RGD4C-hTNF-α and β-actin as a housekeeping gene was performed using hTNF-α primers: 5′-CAGCCTCTTCTCCTTCCTGAT-3′ and 5′-GCCAGAGGGCTGATTAGAGA-3′; β-actin primers and Universal Probe library set (Roche Applied Science) in the LightCycler480 II system (Roche Diagnostics, Mannheim, Germany).

2.11. Immunohistochemical analysis of RGD4C-hTNF-α expression

Tissue samples obtained on day 1 after injection of polyplex micelles were embedded in OCT compounds and frozen in cold acetone. Frozen sections (8–10 μm) were air dried and fixed in cold acetone for 10 min. After blocking with 3% bovine serum albumin (BSA), the sections were incubated with a rat anti-human TNF-α antibody (1:250; MCA1560, AbD Serotec, Kidlington, UK) at room temperature for 1 h, followed by a biotinylated rabbit anti-rat IgG(H + L) (1:250; BA-4001, Vector Laboratories Inc., Burlingame, CA) for 10 min. The sections were stained with horseradish peroxidase-conjugated streptavidin (PK-6100, Vector Laboratories Inc.) and 3,3′-diaminobenzidine (DAB) substrate kit (SK-4100, Vector Laboratories Inc.).

2.12. Histochemical analysis for the in vivo distribution of polyplex micelle

Fluolid Orange NHS (International Science Technology Co. LTD., Fukuoka, Japan) was conjugated to amino groups of polycations, such as PEG-P[Asp(DET)] and PEG-SS-P[Asp(DET)], according to the manufacturer's protocol. Fluolid Orange-labeled polyplex micelles loading pDNA were intraperitoneally injected at a dose of 50 μg/mouse. Mice were sacrificed after 24 h and excised organs were frozen in OCT compounds. The frozen samples were further sectioned at a 10-μm thickness in a cryostat. The nuclei were stained with DAPI. The samples were observed by confocal scanning laser microscopy NIKON A1 (NIKON CORPORATION, Tokyo, Japan).

2.13. Hepatic and renal function tests

Polyplex micelles consisting of pVIVO-RGD4C-hTNF-α (50 μg/mouse, N/P ratio = 10) were intraperitoneally administered to BALB/c mice (female, n = 6). Blood was collected from the vena cava at 4, 24, and 72 h, allowed to coagulate for 4 h at 4 °C and then serum was isolated as the supernatant fraction following centrifugation at 2000 *g* for 10 min.

To assess hepatic and renal toxicities of polyplex micelles, serum concentrations of alanine aminotransferase (ALT) and creatinine were determined by Japan Society of Clinical Chemistry (JSCC) transferable and enzyme methods, respectively, with 7180 Clinical Analyzer (Hitachi, Tokyo, Japan). Body weight changes were monitored as an index of overload influence for whole body.

2.14. Statistical analysis

Results are represented as means ± standard deviation (SD). Data were statistically analyzed using Student's *t*-test. Survival was analyzed by Kaplan–Meier method with a log-lank test. A P value less than 0.05 was considered to represent a statistically significant difference.

3. Results

3.1. Polyplex micelle characterization

As shown in Table 1, the polyplexes from PEG-SS-P[Asp(DET)] and PEG-P[Asp(DET)] formed the micelles in equivalent diameter at the range of 80–90 nm. The polyplex micelles from the block copolymer showed almost neutral ζ-potential values (~2 mV) due to the shielding by a PEG palisade surrounding the polyplex core.

3.2. Kinetics assay for luciferase activity by bioluminescence imaging in vivo

Fig. 2 shows the time-course changes in luciferase activity *in vivo* after intraperitoneal injection of polyplex micelles with the reporter gene. The luciferase activity was elevated with the peak at 24 h after injection ($P<0.05$, each polyplex micelle-treated *versus* control group). The activities were gradually declined, but sustained more than 4.2 and 2.7×10^5 photons/s for PEG-SS-P[Asp(DET)] and PEG-P[Asp(DET)] groups, respectively, on day 7, which were higher ($P<0.05$) than the control ($1.2\pm0.4\times10^5$ photons/s). Next, we compared the level of transgene expression between polyplex micelles. PEG-SS-P[Asp(DET)] exhibited 2-orders of magnitude higher luciferase activity ($1.8\pm1.6\times10^8$ photons/s) than PEG-P[Asp(DET)] ($3.0\pm1.4\times10^6$ photons/s, $P<0.05$) on day 1 after polyplex micelle injection. The luciferase activity was still higher in PEG-SS-P[Asp(DET)] than PEG-P[Asp(DET)] group on days 2 and 4 ($P<0.05$). On day 7 after injection, there was no significant difference between the two groups.

3.3. Transgene expression in tumor and normal organ tissues

Expression levels of therapeutic gene: RGD4C-hTNF-α were evaluated by the qRT-PCR in various tissues (Fig. 3). PEG-SS-P[Asp(DET)] and PEG-P[Asp(DET)] polyplex micelles induced 100-fold higher expression of RGD4C-hTNF-α in tumor nodules compared to the control ($P<0.05$, Fig. 3B). Similarly, each polyplex group showed significantly higher RGD4C-hTNF-α expressions compared to control in some tissues, such as spleen and liver ($P<0.05$, Fig. 3C,D). Other tissues of kidney, lung and intestine showed faint transgene expression (Fig. 3E,F,G).

Next, we compared RGD4C-hTNF-α expression levels between each polyplex micelle. PEG-SS-P[Asp(DET)] polyplex micelles-treatment resulted in 5.0-fold higher ($P=0.028$) expressions of RGD4C-hTNF-α than those of PEG-P[Asp(DET)] in tumor. In spleen and liver, there was no significant difference in RGD4C-hTNF-α expression between PEG-SS-P[Asp(DET)] and PEG-P[Asp(DET)] polyplex micelles.

The expression of RGD4C-hTNF-α protein was also confirmed by immunohistochemical analysis in tumor nodules after administration of the PEG-SS-P[Asp(DET)] and PEG-P[Asp(DET)] polyplex micelles (Fig. 4A). The transduced RGD4C-hTNF-α was detected in tumor tissues, and the localization was predominately detected in peripheral tumor sites. The expression of RGD4C-hTNF-α was also observed in spleen and lymph nodes for PEG-SS-P[Asp(DET)] and PEG-P[Asp(DET)]

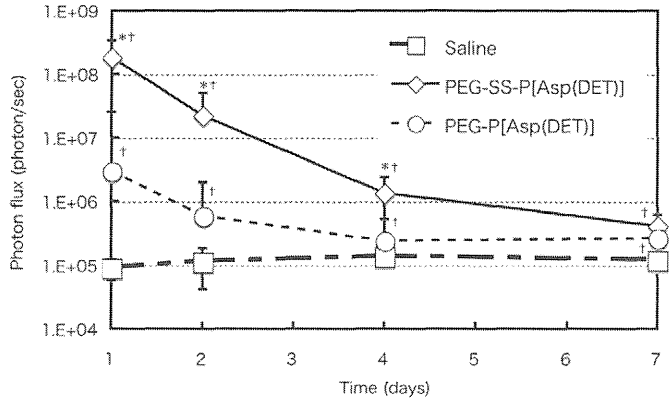

Fig. 2. Luciferase activities after intraperitoneal administration of two types of polyplex micelles loaded with a luciferase gene or saline. The time-dependent changes in luciferase activities were evaluated with an IVIS Imaging System. Saline (□); PEG-SS-P[Asp(DET)](◇); PEG-P[Asp(DET)] (○) (n=6 in each group; * $P<0.05$ *versus* PEG-P[Asp(DET)]; † $P<0.05$ *versus* saline).

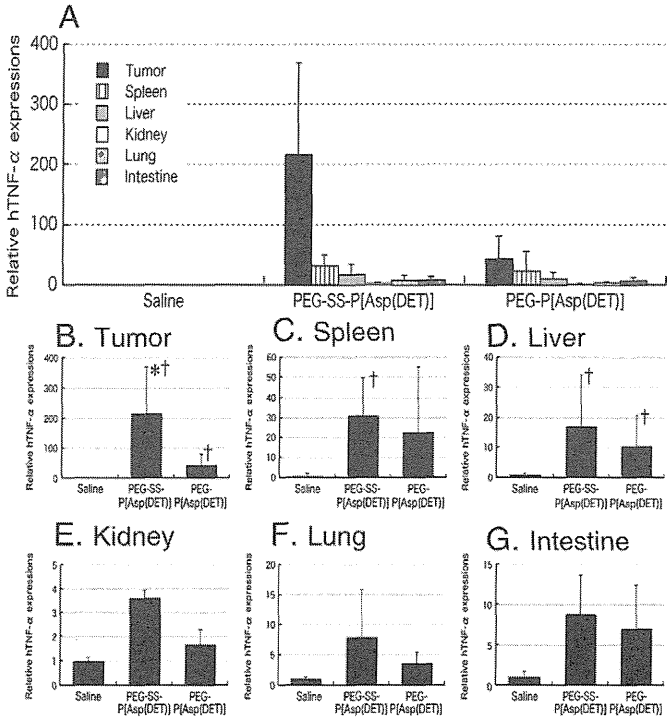

Fig. 3. Evaluation of RGD4C-TNF-α gene expression in organs by qRT-PCR. Saline and two types of polyplex micelles (50 μg pDNA/mouse) were i.p. injected into mice bearing SUIT-2 disseminated cancers. On day 1 after injection, the organ tissues were excised, and the total RNA were extracted and subjected to the quantification of RGD4C-TNF-α expression by qRT-PCR (A). The below graphs represent for tumor (B), spleen (C), liver (D), kidney (E), lung (F) and intestine tissues (G). Results are means ± standard deviations (n=3 in each group; * $P<0.05$ *versus* PEG-P[Asp(DET)]; † $P<0.05$ *versus* saline).

Table 1
Particle size and ζ-potential of polyplex micelles.

	Size (nm)	ζ-potential (mV)
PEG-SS-P[Asp(DET)]	84.7 ± 0.60	1.97 ± 1.16
PEG-P[Asp(DET)]	86.1 ± 0.48	1.55 ± 0.41

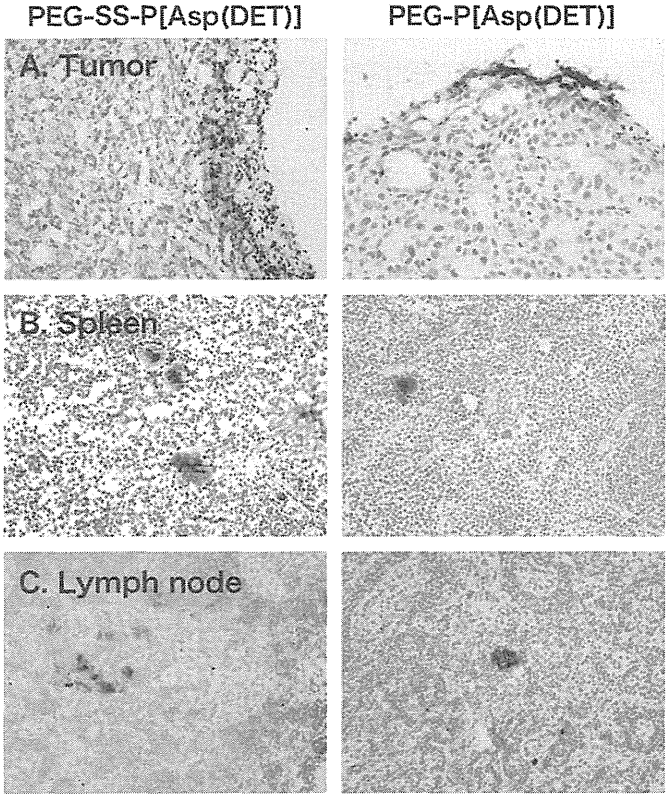

Fig. 4. Immunostaining of RGD4C-hTNF-α in (A) tumor (×10), (B) spleen (×10) and (C) lymph nodes (×20). The polyplex micelles (50 μg pVIVO-RGD4C-hTNF-α pDNA/mouse) were i.p. injected into mice bearing SUIT-2 disseminated cancers. On day 1 after injection, the organs were excised and immunostained with a primary anti-human TNF-α antibody, followed by a secondary anti-rat IgG and a subsequent DAB substrate.

groups (Fig. 4B,C). The RGD4C-hTNF-α signals were located not only in subserous area but also in white pulp of spleen area.

3.4. In vivo distribution of polyplex micelles

The delivered locus of polyplex micelle was analyzed by confocal laser microscopic detection of Fluolid Orange labeled polycation (Fig. 5) in various tissues. There was no significant difference in tissue distribution between PEG-SS-P[Asp(DET)] and PEG-P[Asp(DET)] polyplex micelles. The two types of polyplex micelles were mainly found in stromal regions of tumor tissues at 24 h after i.p. administration (Fig. 5A). Fluolid signals were also detected in the white pulp of the spleen and lymph nodes post administration of PEG-SS-P[Asp(DET)] polyplex micelles as similarly as PEG-P[Asp(DET)] (Fig. 5B). In the liver, Fluolid signals were sparsely observed in hepatic parenchymal area for either polyplex micelle group (Fig. 5C). The kidney, lung, intestine, brain, ovary and heart were not detected for Fluolid signals either in PEG-SS-P[Asp(DET)] or PEG-P[Asp(DET)] groups (data not shown).

3.5. Antitumor activity

To compare the antitumor effect of the polyplex micelles encapsulated with RGD4C-hTNF-α gene, we evaluated the disseminated tumor volume by bioluminescent signals from luciferase-transfectant pancreatic cancers. The changes in relative tumor volume (V/V_0) after single i.p. administration of polyplex micelles are shown in Fig. 6A. The time-dependent increases in tumor volume were observed in the saline-control group (4.7 ± 4.1 on day 7; 48.9 ± 40.3 on day 14; 65.2 ± 63.6 on day 21). The tumor growth was also found in PEG-P[Asp(DET)] group (2.6 ± 1.5 on day 7; 8.0 ± 4.8 on day 14; 44.0 ± 42.2 on day 21), although the growth speed was decreased by PEG-P[Asp(DET)] polyplex micelles-treatment ($P<0.05$). On the other hand, the growth suppression was obviously induced by PEG-SS-P[Asp(DET)] polyplex micelles-treatment (2.2 ± 2.0 on day 7; 2.7 ± 2.3 on day 14; 5.2 ± 2.1 on day 21). There were significant differences in tumor growth between PEG-SS-P[Asp(DET)] group ($P<0.05$), PEG-P[Asp(DET)] and control groups.

We next compared the survival between the polyplex micelles-treated and control mice. The median survival of the PEG-P[Asp(DET)] group was longer than that of control mice (57.3 ± 7.9 *versus* 43.5 ± 7.5 days, $P<0.05$) (Fig. 6B). The survival of the PEG-SS-P[Asp(DET)] group (65.9 ± 6.8 days) was further prolonged ($P<0.05$) than those of PEG-P[Asp(DET)] and control groups.

3.6. Toxicity study of polyplex micelles

The serum ALT concentrations as an index of hepatic toxicity did not increase during the observation time in all groups. There were no differences in ALT between the polyplex micelles-treated, saline and untreated mice (Table 2A). The creatinine concentrations as an index of renal toxicity also did not change, and no significance was observed between the two polyplex group, saline and untreated mice (Table 2B). Body weight was monitored as an indicator of overload influence for whole body. It is clear that each group has no observable side effects at 50 μg pDNA dosage except PEG-SS-P[Asp(DET)] group at 24 h after i.p. administration in this study (Fig. 7).

4. Discussion

A challenging demand in the field of non-viral gene therapy is to provide efficient transduction without significant toxicity. In the present study, we explored the biodistribution, gene expression, therapeutic efficacy and safety potentials of PEG-detachable polyplex micelle as a gene carrier *in vivo* to verify our hypothesis that the PEG release from polycation contributes to the increase in transduction efficiency without toxicity.

PEG-SS-P[Asp(DET)] exhibited higher level of RGD4C-hTNF-α gene expression in tumor tissue than that of PEG-P[Asp(DET)] by qRT-PCR analysis (Fig. 3B). It should be noted that PEG-SS-P[Asp(DET)] reveals almost 2 order of magnitude higher *in vitro* [22] and *in vivo* kinetics study for reporter gene expression than PEG-P[Asp(DET)] (Fig. 2). On the other hand, the distributed location and amount of PEG-SS-P[Asp(DET)] and PEG-P[Asp(DET)] polyplex micelles did not differ remarkably based on the data of Fluolid histochemical analysis (Fig. 5A). These results suggest that the major cause for high transgene expression in tumor with the polyplex micelles from the PEG-SS-P[Asp(DET)] may be not the difference in distributed amount of micelles into tumors. A previous study [22] has reported that confocal laser scanning microscopy shows the facilitated endosomal escape of pDNA with the PEG-SS-P[Asp(DET)] but not much with PEG-P[Asp(DET)] in culture cells. Although the intracellular trafficking of Fluolid in tissues was practically difficult (data not shown), PEG detachment may lead to facilitated transfection in the intracellular stage.

Considering the mechanism of tumor-targetability of polyplex micelles, biodistribution of polyplex micelles should be addressed to several aspects of enhanced permeability and retention (EPR) effect [32] and direct penetration into tumor tissues. Possible route of gene transfer is a direct infiltration of polyplexes to tumor tissues through its surface. The organs in the peritoneal cavity are normally covered with the peritoneum, subperitoneal connective tissue and serosa, whereas the disseminated tumor nodules are devoid of such coverings, since the interaction of cancer cells with the peritoneum induces disruption and exfoliation of the mesothelial cells in the early process of peritoneal metastasis [33,34]. Tumor tissues without such

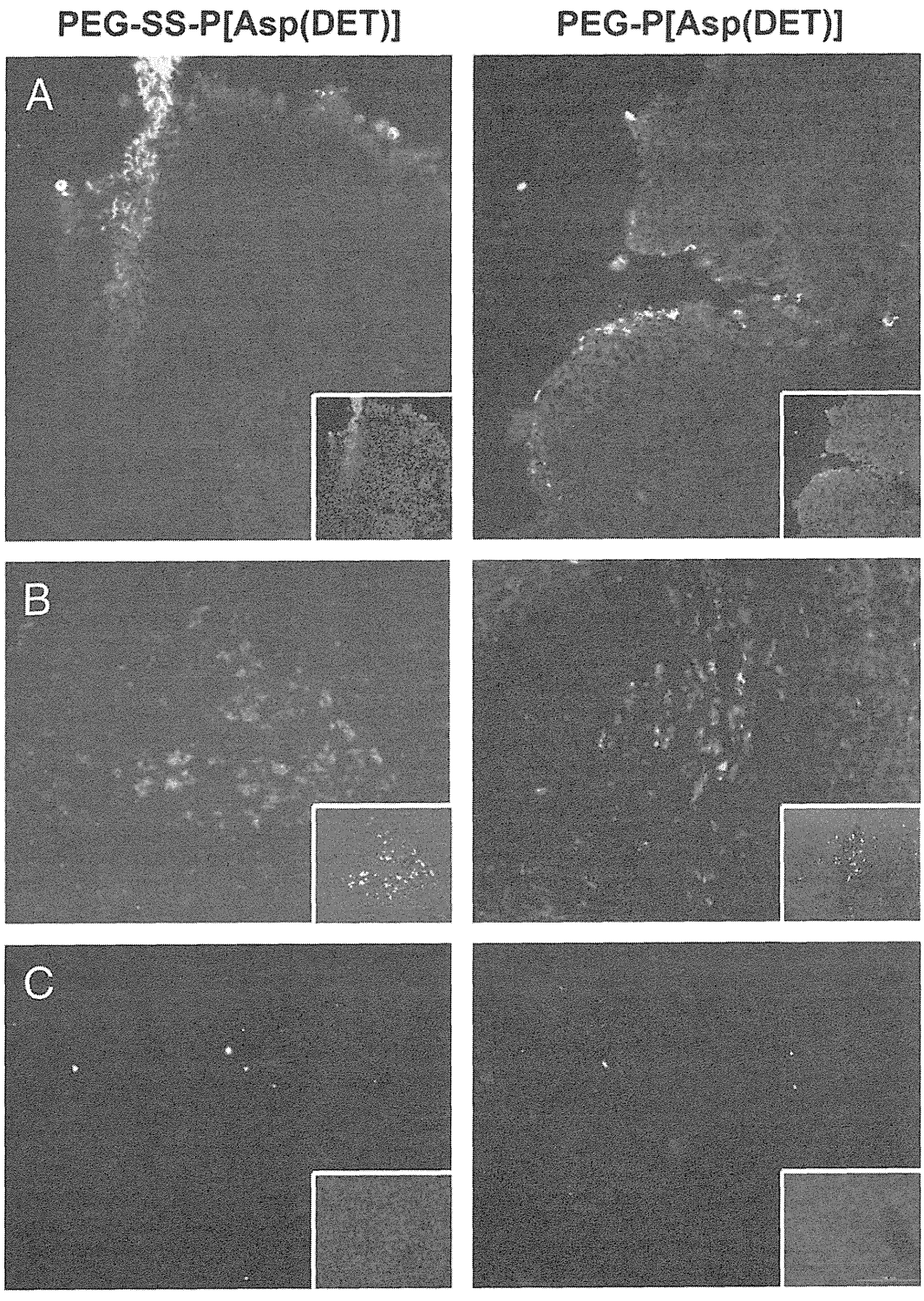

Fig. 5. Polyplex micelle localization in tumor (A), spleen (B) and liver (C). Fluolid Orange-signals labeled polyplex micelles (orange) were detected in tumor and normal organ tissues by laser confocal microscopy at 24 h after polyplex micelle administration. The cell nuclei were stained with DAPI (blue).

barriers could be infiltrated with the polyplexes. Another possible route of gene transfer is a tumor accumulation *via* blood vessels by EPR effect [32]. However, the proportion in tumor accumulation of polyplexes *via* blood vessels might not be dominant, since large molecular compounds (M.W.>20, 000) do not efficiently drain from peritoneal cavity to blood vessels [35,36]. An additional element which may account for the tumor-preference is that the transduced gene is more readily expressed in proliferating cells, such as cancer and inflammatory cells, but little in normal quincent cells [37]. Fig. 3 showed that there are no significant differences in transgene expressions in normal organs between the two types of micelles. The disulfide linkage might be cleaved more effectively in tumor tissues, because tumors are under more reducing conditions compared to normal organs [38]. Since transfected gene is transported to the nucleus inefficiently

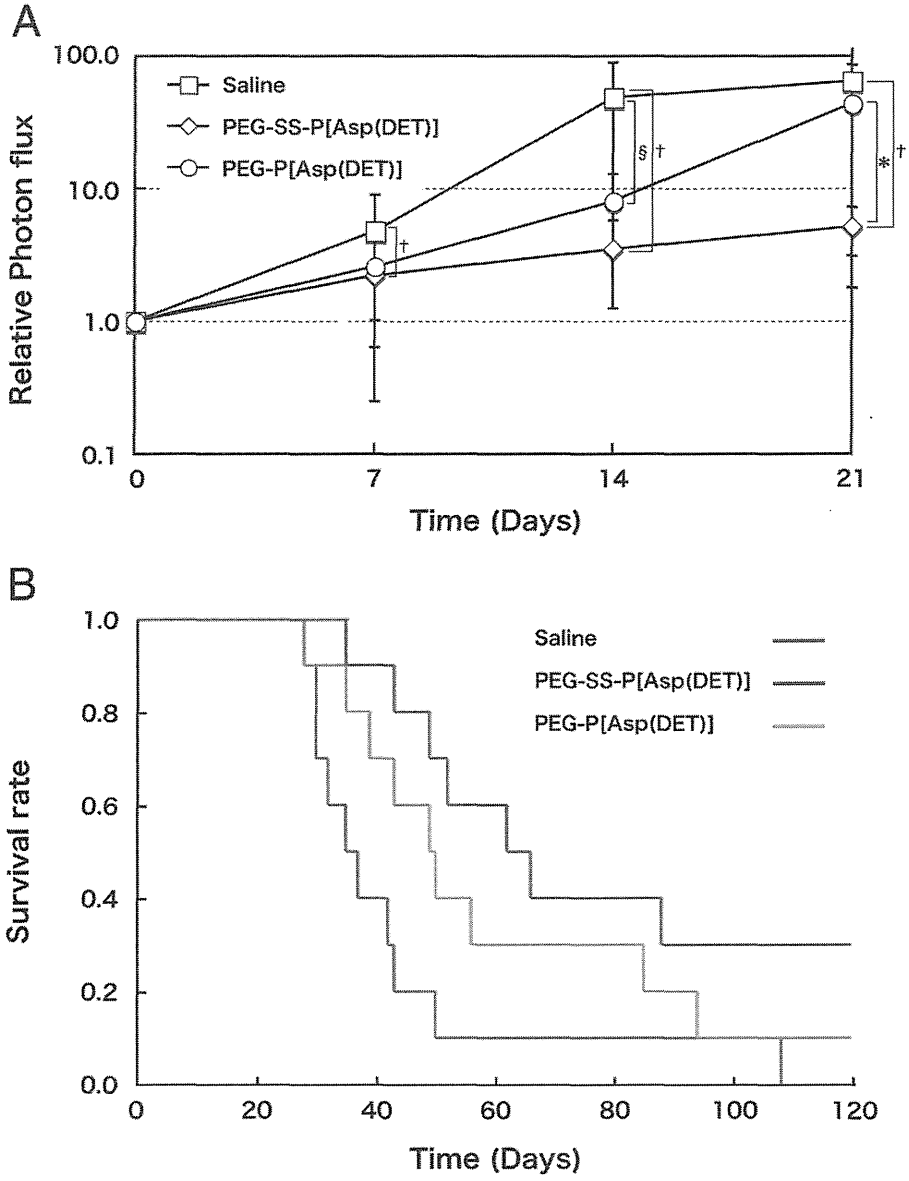

Fig. 6. Antitumor activity of polyplex micelles with pVIVO-RGD4C-hTNF-α pDNA in mice with SUIT-2/luc peritoneal dissemination. (A) Relative photon flux evaluated by IVIS imaging system for intraperitoneal metastatic sites of SUIT-2/luc in mice treated with polyplex micelles. Saline (□); PEG-SS-P[Asp(DET)](◇); PEG-P[Asp(DET)] (○). Data are expressed as averages ± standard deviations (* $P<0.05$ *versus* PEG-P[Asp(DET)]; † $P<0.05$ *versus* saline). (B) Kaplan–Meier analysis for survival of mice bearing peritoneal dissemination that received i.p. injection of saline, PEG-SS-P[Asp(DET)] or PEG-P[Asp(DET)] polyplex micelles.

through the nuclear membrane during interphase, it is likely that the breakdown of the nuclear membrane during cell cycle may be crucial for efficient transgene expression [39,40].

An interesting finding in our fluorescence study is that i.p. administered polyplexes tended to be predominantly delivered into stromal regions of peripheral tumor tissues (Fig. 5A). PEG-SS-P[Asp(DET)] and PEG-P[Asp(DET)] polyplex micelles accumulated in stromal regions but not inside the tumor nests, because high tumor cell density is a barrier of polyplex micelle infiltration. Drug penetration is impeded by severe fibrosis and high interstitial pressure [41–43]. These physiobiological features of tumor nodules are thought to be involved in the unique distribution of polyplex micelles after i.p. injection.

PEG-SS-P[Asp(DET)] and PEG-P[Asp(DET)] polyplex micelles also transduced gene expression in spleen and liver (Fig. 3C, D), while the degree of gene expression and distribution to spleen and liver was similar in both polyplex micelles (Fig. 5B, C). Expression loci were mainly in the inner area, but not in the outer layer area, of the spleen, liver and lymph nodules (Fig. 4B, C). The transgene expression profile in various organs after i.p. injection of the polyplexes is different from that after intravenous injection, in which the lung, liver and kidney appear as preferential expression sites, probably as a consequence of the filtration function of these organs [44–48]. The polyplexes after i.p. injection might enter into the lymphatics and portal blood vessels predominantly and consequently distribute the lymphatic and liver tissue, but minorly into systemic blood circulation to distant organs, such as lung and kidney. Large molecular compounds (M.W. > 20,000) hardly penetrate into normal tissues, whereas they drain to lymphatic systems regardless of size and charge of nanoparticles [35,36]. This property of distribution with lymphatic tropism indicates that the strategy of i.p. administration would be effective to activate immunity in the lymphatic tissues, leading to the application for immuno-gene therapy.

In peritoneal disseminated cancer model, PEG-SS-P[Asp(DET)] polyplex micelles encapsulating pVIVO-RGD4C-hTNF-α plasmid inhibited the proliferation of tumors more effectively compared

Table 2
Evaluation of hepatic and renal toxicity after intraperitoneal administration of two types of polyplex micelles encapsulating pVIVO-RGD4C-hTNF-α. Serum ALT (A) and creatinine (B) levels were measured at 4, 24, and 72 h after i.p. administration of polyplex micelles in mice (n = 6 in each group).

Time (h)	Normal	Saline	PEG-SS-P[Asp(DET)]	PEG-P[Asp(DET)]
(A) ALT				
4	44.6 ± 21.5	53.7 ± 18.0	45.8 ± 21.9	48.0 ± 20.4
24		64.0 ± 31.5	68.0 ± 14.6	56.5 ± 16.1
72		56.0 ± 17.4	48.6 ± 7.8	48.0 ± 9.3
(B) Creatinine				
4	0.14 ± 0.03	0.15 ± 0.01	0.12 ± 0.02	0.13 ± 0.02
24		0.16 ± 0.02	0.16 ± 0.02	0.14 ± 0.03
72		0.15 ± 0.01	0.15 ± 0.02	0.12 ± 0.03

with PEG-P[Asp(DET)] polyplex micelles (Fig. 6A). In addition, PEG-SS-P[Asp(DET)] polyplex micelles significantly prolonged the survival for mice with peritoneal dissemination compared with PEG-P [Asp(DET)] polyplex micelles (Fig. 6B). The antitumor effects might be mediated by paracrine action of RGD4C-TNF-α to tumor and vascular endothelial cells from the polyplex micelles in tumor stroma, although subsets of tumor species gain the resistance to TNF-α [49]. The production level of RGD4C-hTNF-α production from PEG-SS-P [Asp(DET)] polyplex micelles was significantly higher than that from PEG-P[Asp(DET)] polyplex micelles (Fig. 3B). High-dose TNF-α causes destruction of newly formed blood vessels [50] and TNF-α induces a dose-dependent reduction of tumor blood flow [51,52]. TNF-α is also known to activate NK and macrophage cells, which might be partly responsible for the antitumor effect of RGD4C-hTNF-α gene therapy on peritoneal disseminated cancer. Furthermore, we constructed RGD4C-hTNF-α expression plasmid gene to increase the specificity of tumor vessels, because RGD4C peptide moiety specifically binds the integrin $\alpha_v\beta_3$, which is overexpressed on tumor vascular endothelial cells [29]. These evidences suggest that the higher local RGD4C-hTNF-α gene expression produced by PEG-SS-P[Asp(DET)] polyplex micelles eradicate tumor vasculature much more than PEG-P [Asp(DET)] polyplex micelles, resulting in an effective inhibition of the progression of disseminated tumor.

To evaluate the toxicity of polyplex micelles, we performed hepatic and renal function tests in mice at several time points after transduction with RGD4C-hTNF-α expression plasmid. A previous report [53] showed that systemically administered pDNA/cationic liposome complex induced toxicity in the liver mainly and not in the lung. In contrast, the hepatic function of mice treated with PEG-SS-P[Asp(DET)] and PEG-P[Asp(DET)] polyplex micelles encapsulating pVIVO-RGD4C-hTNF-α plasmid were kept normal as similarly as untreated mice (Table 2A). These results indicated that polyplex micelles are not toxic to liver tissues when the current dose was administered *via* i.p., although polyplex micelles were distributed to the liver (Fig. 5C). Secondly, no change in serum creatinine level suggests that PEG-SS-P[Asp(DET)] and PEG-P[Asp(DET)] polyplex micelles induce no nephrotoxicity (Table 2B). This could be explained by the low expression of RGD4C-hTNF-α gene in the kidney (Fig. 3E) due to little distribution of polyplex micelles to this organ (data not shown). This was consistent with the previous report for PEI [54]. Moreover, no significant body weight loss was observed after i.p. administration of polyplex micelles except the transient decrease at 24 h, when surgical and anesthesia stress together with polyplex i.p. irritation might limit the intake of water and food, despite hepatic and renal functions were intact. TNF-α fusion protein has effective antitumor effects by repeated administrations [29], and has been tried for clinical application as an antineoplastic agent [55,56]. However, clinical applications of TNF-α fusion protein for cancer therapy are still limited, because systemic administration of TNF-α protein induces toxic side effects [57,58], such as fever and decreased blood pressure, and the drug concentration at the tumor sites does not reach to the range of therapeutic dose due to the dilution factor after systemic administration [59], although recombinant TNF-α protein might be effective with minimal toxicity when infused by intraperitoneal administration, not by systemic administration. On the other hand, administration of PEG-detachable polyplex micelles encapsulating pVIVO-RGD4C-hTNF-α plasmid showed no remarkable toxic side effects, while the local expression of RGD4C-hTNF-α from the polyplex micelles in tumor stroma leads to sustain the concentration of this cytokine enough to exhibit the antitumor effect, even by single-administration regimen. In addition, TNF-α based gene therapy may have synergistic potential for tumor eradication when combined with ganciclovir suicide gene [60] and irradiation/chemotherapy [61] despite of investigational therapy to date. Our polymeric micelle systems can be also applied for cotransfection with same platform. These results suggest that i.p. administration of PEG-detachable polyplex micelles encapsulating pVIVO-RGD4C-hTNF-α plasmid may have advantages in wide capacity for safety in the diseased condition with peritoneal disseminated tumors.

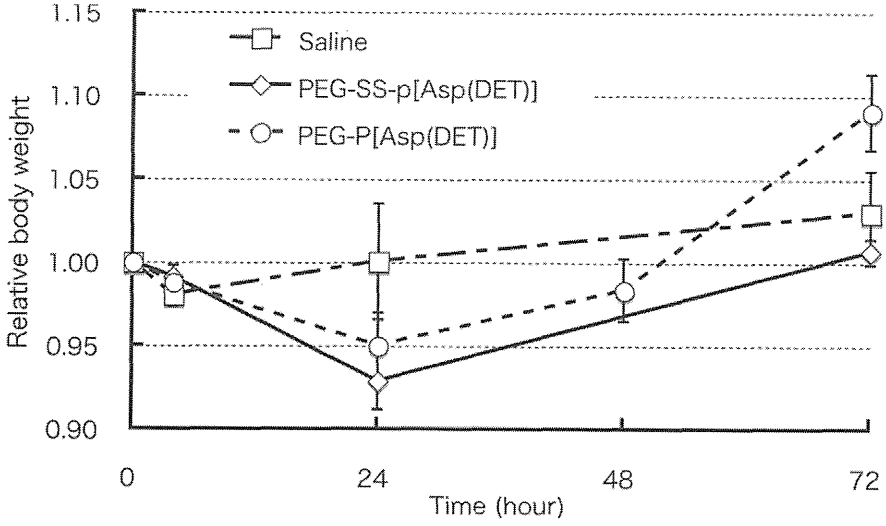

Fig. 7. Changes in body weight of mice treated with two types of polyplex micelles encapsulating pVIVO-RGD4C-hTNF-α. Saline (□); PEG-SS-P[Asp(DET)](◇); PEG-P[Asp(DET)] (○) (n = 6 in each group).

In conclusion, we have demonstrated that PEG-detachable polyplex micelles exhibit an appreciable transgene expression in tumor, spleen and liver without significant toxicity, resulting in the antitumor efficacy for peritoneally disseminated cancer. The safe and effective modality for peritoneal dissemination could be achieved by gene therapy using PEG-detachable polyplex micelles in future clinical applications.

Acknowledgments

This work was financially supported in part by the Grants-in-Aid for Scientific Research to K.N. from the Japanese Ministry of Education, Culture, Sports, Science and Technology, Japan (MEXT) (project code: 21390374). This research is also partly supported by the Funding Program for World-Leading Innovation R&D on Science and Technology (FIRST Program) from the Japan Society for the Promotion of Science (JSPS), initiated by the Council for Science and Technology Policy (CSTP), and the Core Research Program for Evolutional Science and Technology (CREST) from Japan Science and Technology Agency (JST). We appreciate Mrs. Michiko Fujita (The University of Tokyo), Mrs. Aya Sakai and Mr. Takaaki Kanemaru (Kyushu University) for technical assistance.

Appendix A. Supplementary data

Supplementary data to this article can be found online at doi:10.1016/j.jconrel.2012.03.021.

References

[1] M.A. Kay, State-of-the-art gene based therapies: the road ahead, Nat. Rev. Genet. 12 (5) (2011) 316–328.
[2] F. Mingozzi, K.A. High, Therapeutic *in vivo* gene transfer for genetic disease using AAV: progress and challenges, Nat. Rev. Genet. 12 (5) (2011) 341–355.
[3] D.W. Pack, A.S. Hoffman, S. Pun, P.S. Stayton, Design and development of polymers for gene delivery, Nat. Rev. Drug Discov. 4 (7) (2005) 581–593.
[4] T. Merdan, J. Kopecek, T. Kissel, Prospects for cationic polymers in gene and oligonucleotide therapy against cancer, Adv. Drug Deliv. Rev. 54 (2002) 715–758.
[5] M. Meyer, E. Wagner, Recent developments in the application of plasmid DNA-based vectors and small interfering RNA therapeutics for cancer, Hum. Gene Ther. 17 (11) (2006) 1062–1076.
[6] T.G. Park, J.H. Jeong, S.W. Kim, Current status of polymeric gene delivery systems, Adv. Drug Deliv. Rev. 58 (4) (2006) 467–486.
[7] K. Osada, R.J. Christie, K. Kataoka, Polyemric micelles from poly(ethylene glycol)-poly(amino acid) block copolymer for drug and gene delivery, J. R. Soc. Interface 6 (Suppl. 3) (2009) S325–S339.
[8] M. Neu, D. Fischer, T. Kissel, Recent advances in rational gene transfer vector design based on poly(ethylene imine) and its derivatives, J. Gene Med. 7 (8) (2005) 992–1009.
[9] S. Katayose, K. Kataoka, Water-soluble polyion complex associates of DNA and poly(ethylene glycol)-poly(L-lysine) block copolymer, Bioconjug. Chem. 8 (5) (1997) 702–707.
[10] S. Katayose, K. Kataoka, Remarkable increase in nuclease resistance of plasmid DNA through supramolecular assembly with poly(ethylene glycol)-poly(L-lysine) block copolymer, J. Pharm. Sci. 87 (2) (1998) 160–163.
[11] M. Ogris, S. Brunner, S. Schuller, S. Kircheis, E. Wagner, PEGylated DNA/transferring-PEI complexes: reduced interaction with blood components, extended circulation in blood and potential for systemic gene delivery, Gene Ther. 6 (4) (1999) 595–605.
[12] K.Y. Kwok, D.L. McKenzie, D.L. Evers, K.G. Rice, Formulation of highly soluble poly(ethylene glycol)-peptide DNA condensates, J. Pharm. Sci. 88 (10) (1999) 996–1003.
[13] K. Itaka, K. Yamauchi, A. Harada, K. Nakamura, H. Kawaguchi, K. Kataoka, Polyion complex micelles from plasmid DNA and poly(ethylene glycol)-poly(L-lysine) block copolymer as serum-tolerable polyplex system: physicochemical properties of micelles relevant to gene transfection efficiency, Biomaterials 24 (24) (2003) 4495–4506.
[14] K. Itaka, A. Harada, K. Nakamura, H. Kawaguchi, K. Kataoka, Evaluation by fluorescence energy transfer of the stability of nonviral gene delivery vectors under physiological conditions, Biomacromolecules 3 (4) (2002) 841–845.
[15] N. Kanayama, S. Fukushima, N. Nishiyama, K. Itaka, W.D. Jang, K. Miyata, Y. Yamasaki, U.I. Chung, K. Kataoka, A PEG-based biocompatible block catiomer with high buffering capacity for the construction of polyplex micelles showing efficient gene transfer toward primary cells, ChemMedChem 1 (4) (2006) 439–444.
[16] D. Akagi, M. Oba, H. Koyama, N. Nishiyama, S. Fukushima, T. Miyata, H. Nagawa, K. Kataoka, Biocompatible micellar nanovectors achieve efficient gene transfer to vascular lesions without cytotoxicity and thrombus formation, Gene Ther. 14 (13) (2007) 1029–1038.
[17] K. Itaka, S. Ohba, K. Miyata, H. Kawaguchi, K. Nakamura, T. Takato, U.I. Chung, K. Kataoka, Bone regeneration by regulated *in vivo* gene transfer using biocompatible polyplex nanomicelles, Mol. Ther. 15 (9) (2007) 1655–1662.
[18] M. Han, Y. Bae, N. Nishiyama, K. Miyata, M. Oba, K. Kataoka, Transfection study using multicellular tumor spheroids for screening non-viral polymeric gene vectors with low cytotoxicity and high transfection efficiencies, J. Control. Release 121 (1–2) (2007) 38–48.
[19] B. Brissault, A. Kichler, C. Leborgne, O. Danos, H. Cheradame, J. Gau, L. Auvray, C. Guis, Synthesis, characterization, and gene transfer application of poly(ethylene glycol-b-ethyleneimine) with high molar mass polyamine block, Biomacromolecules 7 (10) (2006) 2863–2870.
[20] M. Kursa, G.F. Walker, V. Roessler, M. Ogris, W. Roedl, R. Kircheis, E. Wagner, Novel shielded transferring-polyethylene glycol-polyethyleneimin/DNA complexes for systemic tumor-targeted gene transfer, Bioconjug. Chem. 14 (1) (2003) 222–231.
[21] K. Sagara, S.W. Kim, A new synthesis of galactose-poly(ethylene glycol)-polyethyleneimine for gene delivery to hepatocytes, J. Control. Release 79 (1–3) (2002) 271–281.
[22] S. Takae, K. Miyata, M. Oba, T. Ishii, N. Nishiyama, K. Itaka, Y. Yamasaki, H. Koyama, K. Kataoka, PEG-detachable polyplex micelles on disulfide-linked block catiomers as bioresponsive nonviral gene vectors, J. Am. Chem. Soc. 130 (18) (2008) 6001–6009.
[23] C. Brigand, C. Arvieux, F.N. Gilly, O. Glehen, Treatment of peritoneal carcinomatosis in gastric cancers, Dig. Dis. 22 (4) (2004) 366–373.
[24] E.D. Tetzlaff, P. Cen, J.A. Ajani, Emerging drugs in the treatment of advanced gastric cancer, Expert Opin. Emerg. Drugs 13 (1) (2008) 135–144.
[25] P. Jacquet, P.H. Sugarbaker, Peritoneal-plasma barrier, Cancer Treat. Res. 82 (1996) 53–63.
[26] T. Kamei, J. Kitayama, H. Yamaguchi, D. Soma, S. Emoto, T. Konno, K. Ishihara, H. Ishigami, S. Kaisaki, H. Nagawa, Spatial distribution of intraperitoneally administered paclitaxel nanoparticles solubilized with poly(2-methacryloxyethyl phosphorylcholine-co-n-butyl methacrylate) in peritoneal metastatic nodules, Cancer Sci. 102 (1) (2011) 200–205.
[27] S. Mocellin, C.R. Rossi, P. Pilati, D. Nitti, Tumor necrosis factor, cancer and anticancer therapy, Cytokine Growth Factor Rev. 16 (1) (2005) 35–53.
[28] H. Wang, Z. Yan, J. Shi, W. Han, Y. Zhang, Expression, purification, and characterization of a neovasculature targeted rmfTNF-α in *Escherichia coli*, Protein Expr. Purif. 45 (1) (2006) 60–65.
[29] H. Wang, K. Chen, W. Cai, Z. Li, L. He, A. Kashefi, X. Chen, Integrin-targeted imaging and therapy with RGD4C-TNF fusion protein, Mol. Cancer Ther. 7 (5) (2008) 1044–1053.
[30] Y. Akiyama, H. Otsuka, Y. Nagasaki, M. Kato, K. Kataoka, Selective synthesis of heterobifunctional poly(ethylene glycol) derivatives containing both mercapto and acetal terminals, Bioconjug. Chem. 11 (6) (2000) 947–950.
[31] M. Mitsui, M. Nishikawa, L. Zang, M. Ando, K. Hattori, Y. Takahashi, Y. Watanabe, Y. Takakura, Effect of the content of unmethylated CpG dunucleotides in plasmid DNA on the sustainability of transgene expression, J. Gene Med. 11 (5) (2009) 435–443.
[32] Y. Matsumura, H. Maeda, A new concept for macromolecular therapeutics in cancer chemotherapy: mechanism of tumoritropic accumulation of proteins and the antitumor agent smancs, Cancer Res. 46 (12) (1986) 6387–6392.
[33] Y. Kiyasu, S. Kaneshima, S. Koga, Morphogenesis of peritoneal metastasis in human gastric cancer, Cancer Res. 41 (3) (1981) 1236–1239.
[34] M.J. Niedbala, K. Crickard, R.J. Bernacki, Interaction of human ovarian tumor cells with human mesothelial cells grown on extracellular matrix. An *in vitro* model system for studying tumor cell adhesion and invasion, Exp. Cell Res. 160 (2) (1985) 499–513.
[35] K. Hirano, C.A. Hunt, Lymphatic transport of liposome-encapsulated agents: effects of liposome size following intraperitoneal administration, J. Pharm. Sci. 74 (9) (1985) 915–921.
[36] K. Hirano, C.A. Hunt, A. Strubbe, R.D. MacGregor, Lymphatic transport of liposome-encapsulated drugs following intraperitoneal administration — effect of lipid composition, Pharm. Res. 6 (1985) 271–278.
[37] A. Kikuchi, Y. Aoki, S. Sugaya, T. Serikawa, K. Takakuwa, K. Tanaka, N. Suzuki, H. Kikuchi, Development of novel cationic liposomes for efficient gene transfer into peritoneal disseminated tumor, Hum. Gene Ther. 10 (6) (1999) 947–955.
[38] G.K. Balendiran, R. Dabur, D. Fraser, The role of glutathione in cancer, Cell Biochem. Funct. 22 (6) (2004) 343–352.
[39] F. Labat-Moleur, A.M. Steffan, C. Brisson, H. Perron, O. Feugeas, P. Furstenberger, F. Oberling, E. Brambilla, J.P. Behr, An electron microscopy study into the mechanism of gene transfer with lipopolyamines, Gene Ther. 3 (11) (1996) 1010–1017.
[40] M. Wilke, E. Fortunati, M. van den Broek, A.T. Hoogeveen, B.J. Scholte, Efficacy of a peptide-based gene delivery system depends on mitotic activity, Gene Ther. 3 (12) (1996) 1133–1142.
[41] A.I. Minchinton, I.F. Tannock, Drug penetration in solid tumors, Nat. Rev. Cancer 6 (8) (2006) 583–592.
[42] M. Yashiro, Y.S. Chung, S. Nishimura, T. Inoue, M. Soma, Fibrosis in the peritoneum induced by scirrhous gastric cancer cells may act as "soil" for peritoneal dissemination, Cancer 77 (8 Suppl.) (1996) 1668–1675.
[43] R.K. Jain, Barriers to drug delivery in solid tumor, Sci. Am. 271 (1) (1994) 58–65.
[44] J.L. Coll, P. Chollet, E. Brambilla, D. Desplanques, J.P. Behr, M. Favrot, *In vivo* delivery to tumors of DNA complexed with linear polyethylenimine, Hum. Gene Ther. 10 (10) (1999) 1659–1666.
[45] D. Goula, C. Benoist, S. Mantero, G. Merlo, G. Levi, B.A. Demeneix, Polyethylenimine-based intravenous delivery of transgenes to mouse lung, Gene Ther. 5 (9) (1998) 1291–1295.
[46] A. Bragonzi, A. Boletta, A. Biffi, A. Muggia, G. Sersale, S.H. Cheng, C. Bordignon, B.M. Assael, M. Conese, Comparison between cationic polymers and lipids in mediating systemic gene delivery to the lungs, Gene Ther. 6 (12) (1999) 1995–2004.

[47] S.M. Zou, P. Erbacher, J.S. Remy, J.P. Behr, Systemic linear polyethylenimine (L-PEI)-mediated gene delivery in the mouse, J. Gene Med. 2 (2) (2000) 128–134.
[48] I. Chemin, D. Morsdour, S. Wieland, W.B. Offensperger, E. Walter, J.P. Behr, H.E. Blum, Liver-directed gene transfer: a linear polyethlenimine derivative mediates highly efficient DNA delivery to primary hepatocytes *in vitro* and *in vivo*, J. Viral Hepat. 5 (6) (1998) 369–375.
[49] V.A. Polunovsky, C.H. Wendt, D.H. Ingbar, M.S. Peterson, P.B. Bitterman, Induction of endothelial cell apoptosis by TNF alpha: modulation by inhibitors of protein synthesis, Exp. Cell Res. 214 (2) (1994) 584–594.
[50] L.F. Fajardo, H.H. Kwan, J. Kowalski, S.D. Prionas, A.C. Allison, Dual role of tumor necrosis factor-alpha in angiogenesis, Am. J. Pathol. 140 (3) (1992) 539–544.
[51] N. Watanabe, Y. Niitsu, H. Umeno, H. Kuriyama, H. Neda, N. Yamauchi, M. Maeda, I. Urushizaki, Toxic effect of tumor necrosis factor on tumor vasculature in mice, Cancer Res. 48 (8) (1988) 2179–2183.
[52] P.L. Naredi, P.G. Linder, S.B. Holmberg, U. Stenram, A. Peterson, L.R. Hafstrom, The effects of tumour necrosis factor alpha on the vascular bed and blood flow in an experimental rat hepatoma, Int. J. Cancer 54 (4) (1993) 645–649.
[53] S. Loisel, C.L. Gall, L. Doucet, C. Ferec, V. Flock, Contribution on plasmid DNA to hepatotoxicity after systemic administration of polyplexes, Hum. Gene Ther. 12 (6) (2001) 685–696.
[54] K. Aoki, S. Furuhata, K. Hatanaka, M. Maeda, J.S. Remy, J.-P. Behr, M. Terada, T. Yoshida, Polyethyleneimine-mediated gene transfer into pancreatic tumor dissemination in the murine peritoneal cavity, Gene Ther. 8 (7) (2001) 508–514.
[55] M. Blick, S.A. Sheriwin, M. Rosenblum, J. Gutterman, Phase I study of recombinant tumor necrosis factor in cancer patients, Cancer Res. 47 (11) (1987) 2986–2989.
[56] P.J. Creaven, J.E. Plager, S. Dupere, R.P. Huben, H. Takita, A. Mittelman, A. Proefrock, Phase I clinical trial of recombinant human tumor necrosis factor, Cancer Chemother. Pharmacol. 20 (2) (1987) 137–144.
[57] T. Moritz, N. Niederle, J. Baumann, D. May, E. Kurschel, R. Osieka, J. Kempeni, E. Svhlick, C.G. Schmidt, Phase I study of recombinant human tumor necrosis factor alpha in advanced malignant disease, Cancer Immunol. Immunother. 29 (2) (1989) 144–150.
[58] W.L. Furman, D. Strother, K. McClain, B. Bell, B. Leventhal, C.B. Pratt, Phase I clinical trial of recombinant human tumor necrosis factor in children with refractory solid tumors: a pediatric oncology group study, J. Clin. Oncol. 11 (11) (1993) 2205–2210.
[59] S.A. Rosenberg, Gene therapy for cancer, J. Am. Med. Assoc. 268 (17) (1992) 2416–2419.
[60] S. Moriuchi, T. Oligino, D. Krisky, P. Marconi, D. Fink, J. Cohen, J.C. Glorioso, Enhanced tumor cell killing in the presence of ganciclovir by herpes simplex virus type 1 vector-directed coexpression of human tumor necrosis factor-α and herpes simplex virus thymidine kinase, Cancer Res. 58 (24) (1998) 5731–5737.
[61] B. Yamini, X. Yu, P. Pytel, N. Galanopoulos, V. Rawlani, J. Veerapong, K. Bickenbach, R.R. Weichselbaum, Adenovirally delivered tumor necrosis factor-α improves the antiglioma efficacy of concomitant radiation and temozolomide therapy, Clin. Cancer Res. 13 (20) (2007) 6217–6223.

Journal of Controlled Release 160 (2012) 542–551

Contents lists available at SciVerse ScienceDirect

Journal of Controlled Release

journal homepage: www.elsevier.com/locate/jconrel

Effective transgene expression without toxicity by intraperitoneal administration of PEG-detachable polyplex micelles in mice with peritoneal dissemination

Michiaki Kumagai [a], Shinya Shimoda [a], Rie Wakabayashi [a], Yumi Kunisawa [a], Takehiko Ishii [b], Kensuke Osada [c], Keiji Itaka [d], Nobuhiro Nishiyama [d], Kazunori Kataoka [c], Kenji Nakano [a,*]

[a] Innovation Center for Medical Redox Navigation, Kyushu University, 3-1-1 Maidashi, Higashi-ku, Fukuoka, Fukuoka 812-8582 Japan
[b] Department of Bio Engineering, Graduate School of Engineering, The University of Tokyo, 7-3-1 Hongo, Bunkyo-ku, Tokyo 113-0033, Japan
[c] Department of Materials Engineering, Graduate School of Engineering, The University of Tokyo, 7-3-1 Hongo, Bunkyo-ku, Tokyo 113-0033, Japan
[d] Division of Clinical Biotechnology, Center for Disease Biology and Integrative Medicine, Graduate School of Medicine, The University of Tokyo, 7-3-1 Hongo, Bunkyo-ku, Tokyo 113-0033, Japan

ARTICLE INFO

Article history:
Received 11 November 2011
Accepted 23 March 2012
Available online 30 March 2012

Keywords:
Polyplex micelle
Disulfide linkage
Gene delivery
Peritoneal dissemination
Intraperitoneal administration

ABSTRACT

Block copolymer of poly(ethylene glycol)-*block*-poly{N-[N-(2-aminoethyl)-2-aminoethyl]aspartamide} (PEG-P[Asp(DET)]) has been originally introduced as a promising gene carrier by forming a nanomicelle with plasmid DNA. In this study, the polyplex micelle of PEG-SS-P[Asp(DET)], which disulfide linkage (SS) between PEG and cationic polymer can detach the surrounding PEG chains upon intracellular reduction, was firstly evaluated with respect to *in vivo* transduction efficiency and toxicity in comparison to that of PEG-P[Asp(DET)] in peritoneally disseminated cancer model. Intraperitoneal (i.p.) administration of PEG-SS-P[Asp(DET)] polyplex micelles showed a higher ($P<0.05$) transgene expression compared with PEG-P[Asp(DET)] in tumors. In contrast, the delivered distribution of the micelles was not different between the two polyplex micelles. PEG-SS-P[Asp(DET)] micelle encapsulating human tumor necrosis factor α (hTNF-α) gene exhibits a higher antitumor efficacy against disseminated cancer compared with PEG-P[Asp(DET)] or saline control. No hepatic and renal toxicities were observed by the administration of polyplex micelles. In conclusion, PEG-detachable polyplex micelles may represent an advantage in gene transduction *in vivo* over PEG-undetachable polyplex micelles after i.p. administration for peritoneal dissemination of cancer.

1. Introduction

Gene therapy has attracted much attention as a promising modality to treat intractable diseases, such as genetic disorder, neurodegenerating disease and cancer [1,2]. Viral vectors, such as adenovirus vector, have been vigorously explored in these strategies, because the gene transfer efficiency is generally higher than nonviral gene vector. However, the clinical use of viral vectors has considerable limitations with respect to safety, and it is desirable to develop a nonviral vector. Recently, PEG-based cationic polymers (catiomers) have been expected as one of promising alternatives to viral gene vectors [3–8]. The block catiomers spontaneously associate with plasmid DNA (pDNA) to form sub-100 nm polyplex micelles with high colloidal stability by hydrophilic PEG palisade surrounding the core under physiological conditions and substantial transfection activity [9–14].

We have demonstrated that polyplex micelles formed by PEG-*block*-poly(aspartamide) copolymers carrying the *N*-(2-aminoethyl)-2-aminoethyl group in the side chain (PEG-P[Asp(DET)]) exhibit high efficiency and low cytotoxicity [15]. The polyplex micelles demonstrated appreciable gene transfer into vascular lesions in animal model [16] and bone defect in animal models [17]. To further achieve successful *in vivo* gene therapy, we have tried to modify the block copolymer, because P[Asp(DET)] homopolymer polyplexes show higher transfection efficiency than PEG-P[Asp(DET)] micelles [18] and the PEG palisade surrounding P[Asp(DET)] cores hampers the gene transfection (PEG dilemma) [19–21]. To overcome the dilemma, we have developed PEG detachable polyplex micelles with disulfide linkages between PEG and P[Asp(DET)], which are sensitive to the intracellular reducing environment [22]. This micelle showed higher gene transfection efficiency than the micelle without disulfide linkages by several orders of magnitude *in vitro* assay [22]. However, the transduction on efficacy and safety for *in vivo* application remains to be evaluated.

Systemic chemotherapy is mainly conducted for the patients bearing refractory advanced malignancies, such as liver or lung metastasis and peritoneal dissemination [23,24]. Among these metastases, peritoneal lesions exhibit relative resistance to systemic chemotherapy due to peritoneal-plasma barrier, which prevents the effective drug delivery from blood vessels into the peritoneal lesions

* Corresponding author. Tel.: +81 92 642 6209; fax: +81 92 642 6024.
E-mail address: kenakano@med.kyushu-u.ac.jp (K. Nakano).

0168-3659/$ – see front matter © 2012 Elsevier B.V. All rights reserved.
doi:10.1016/j.jconrel.2012.03.021

[25]. In comparison with conventional systemic chemotherapy, the intraperitoneal (i.p.) administration of hydrophobic chemotherapeutic agents or vectors encapsulated therapeutic genes appears to have an advantage for peritoneal dissemination, because the drugs are directly delivered into the peritoneal cavity and retarded in tumor nodules, which enables to keep high dose concentration in tumor tissues [26]. In addition, gene therapy prevents the rapid enzymatic degradation of therapeutic molecules, such as tumor necrosis factor α (TNF-α), which is known to exhibit anti-tumor effect for a wide variety of cancers [27], and the inflammation-related toxicity induced by its systemic administration of high dose cytokines, although tumor vasculature-specific ligands could increase an accumulation of RGD4C-TNF-α into tumor vicinities [28,29].

In this study, we examined the feasibility of PEG detachable polyplex micelles on transduction efficiency, therapeutic efficacy and safety as a gene delivery system compared with the conventional polyplex without disulfide linkage. The intraperitoneal administration of PEG-detachable polyplex micelles with RGD4C-TNF-α-encoding plasmid, but not that of PEG-undetachable polyplex, revealed an appreciable *in vivo* gene expression and antitumor effect against peritoneal metastases of pancreatic cancer, despite of no difference in the preferable distribution for tumor and lymphatic tissues.

2. Materials and methods

2.1. Chemicals

α-Methoxy-ω-hydroxyl PEG (PEG-OH, $M_n = 12{,}000$, $M_w/M_n = 1.03$) β-benzyl L-aspartate *N*-carboxyanhydride (BLA-NCA) were obtained from NOF Corporation (Tokyo, Japan) and Chuo Kaseihin Co., Inc. (Tokyo, Japan). Methanol (MeOH), 2-aminoethanethiol, diethyl ether, ammonia (NH_3), hexane, ethyl acetate (AcOEt), and hydrochloric acid (HCl) were purchased from Wako Pure Chemical Industries, Ltd. (Osaka, Japan) and used as received. Dichloromethane (CH_2Cl_2), *N,N*-dimethylformamide (DMF), diethylenetriamine (DET) and *N*-methyl-2-pyrrolidone (NMP) were purchased from Tokyo Chemical Industry Co. Ltd. (Tokyo, Japan) or Nacalai Tesque (Kyoto, Japan) and purified by distillation before use. Linear polyethyleneimine (LPEI, $M_w = 22{,}000$) was purchased from Polysciences, Inc. (Warrington, PA). Water was purified using a Milli-Q instrument (Millipore, Bedford, MA).

2.2. Synthesis and characterization of PEG-SS-P[Asp(DET)]

PEG-SS-P[Asp(DET)] was prepared as previously reported [22] with minor modification. Briefly, PEG-OH was converted to PEG-SH [30], of which conversion rate was estimated as 80% from ^{1}H NMR spectrum. The crude PEG-SH (0.85 g) was dissolved in MeOH (30 mL), followed by the reaction with 2-aminoethanethiol (100 equiv, 0.65 g) at room temperature to obtain PEG-SS-NH_2. The polymer components were precipitated into an excess amount of diethyl ether, and then the filtrate was dried *in vacuo*. PEG-SS-NH_2 was isolated from the crude product by passing through an ion-exchange gel (SP Sephadex C-50, GE Healthcare, Tokyo, Japan) column. Adsorbed PEG-SS-NH_2 was eluted from the gel by diluted NH_3 aqueous solution, evaporated using rotary evaporator at 30 °C, and then lyophilized as a white powder (0.63 g in yield). The functionality of the PEG end to the aminoethanethiol moiety was confirmed to be 97% by an ion-exchange HPLC equipped with TSKgel SP-5PW column (TOSOH Corporation, Tokyo, Japan).

The PEG-SS-poly(β-benzyl L-aspartate) (PEG-SS-PBLA) block copolymer was prepared by the ring opening polymerization of BLA-NCA (3.3 mmol, 0.97 g) in CH_2Cl_2/DMF (10/1 (v/v), 23 mL) at 35 °C from the terminal primary amino group of PEG-SS-NH_2 (0.04 mmol, 0.50 g). The reaction mixture was added into an excess amount of hexane/AcOEt (6/4 (v/v)), and then the filtrate was dried *in vacuo* (1.17 g in yield). The degree of polymerization (DP) of PBLA was calculated to be 69 by ^{1}H NMR spectroscopy based on the peak intensity of benzyl protons of PBLA ($-OCH_2C_6H_5$, $\delta = 7.3$ ppm) to the ethylene protons in PEG ($-OCH_2CH_2$, $\delta = 3.6$ ppm).

Lyophilized PEG-SS-PBLA (230 mg) was dissolved in NMP (9 mL), followed by the reaction with DET (4 mL, 50 equiv to benzyl group of PBLA segment), diluted in NMP (4 mL) under anhydrous conditions at 5 °C. After 30 min, the reaction mixture was slowly added dropwise into a 5 N HCl aqueous solution, where the temperature of the mixture was kept below 5 °C. Then the mixture was dialyzed against 0.01 N HCl and, subsequently, deionized water (MWCO: 12–14 kDa) at 4 °C. The final solution was lyophilized to obtain PEG-SS-P[Asp(DET)] (Fig. 1) as the chloride salt form (213 mg in yield). The quantitative substitution from BLA to Asp(DET) was confirmed by the peak disappearance of benzyl protons ($-OCH_2C_6H_5$, $\delta = 7.3$ ppm) and the intensity ratio of the ethylene protons in the 1,2-diaminoethani moiety ($H_2N(CH_2)_2NH(CH_2)_2NH$-, $\delta = 3.4$–2.8 ppm) to the methylene protons in PEG ($-OCH_2CH_2$, $\delta = 3.6$ ppm) in the ^{1}H NMR spectrum in D_2O (data not shown).

2.3. Plasmid DNA construction

A plasmid encoding luciferase (pCpG-ΔLuc) was kindly supplied from Dr. Makiya Nishikawa (Kyoto University) [31]. As expression plasmids encoding therapeutic gene, pVIVO-RGD4C-hTNF-α and pCpG-RGD4C-hTNF-α were constructed as follows; the oligonucleotide encoding RGD4C (CDCRGDCFC) with glycine–serine linker interposed between RGD4C and matured human TNF-α (hTNF-α) sequences as a spacer was synthesized. The open-read frame of RGD4C-hTNF-α was integrated at the multi-cloning sites in the plasmid DNA of pVIVO1-mcs with hamster 78-kDa glucose-regulated protein (GRP78) promoter which yields persistent high expression within the tumor micro-environment or in the plasmid of pCpGfree-mcs to delete immunogenic CpG motifs with human elongation factor 1 alpha core promoter (Invivogen, San Diego, CA). The plasmid DNA was amplified in competent DH5R *Escherichia coli* and purified using EndoFree Plasmid Giga Kits (QIAGEN Inc., Valencia, CA). The pDNA concentration was determined by reading the absorbance at 260 nm.

2.4. Preparation of PEG-SS-P[Asp(DET)]/pDNA polyplex micelles

The PEG-SS-P[Asp(DET)] block copolymer and pDNA were separately dissolved in 10 mM Tris–HCl buffer (pH 7.4). The polymer solution was added to a 2-times-excess volume of 375 μg/mL pDNA solution (final pDNA concentration: 250 μg/mL) at N/P ratio = 10, which is a molar ratio of amine units in block catiomers to phosphate units in pDNA. The mixed solution was left at 4 °C for 15 min to form polyplex micelles and then subjected to the following experiments. Just prior to *in vivo* administration, 1/10 volume of 1.5 M NaCl solution was added to form isotonic solution. The polyplexes with PEG-P[Asp(DET)] block copolymer (*M*w of PEG: 12,000; DP of P[Asp(DET)] segment: 65) or LPEI were similarly prepared and used as controls.

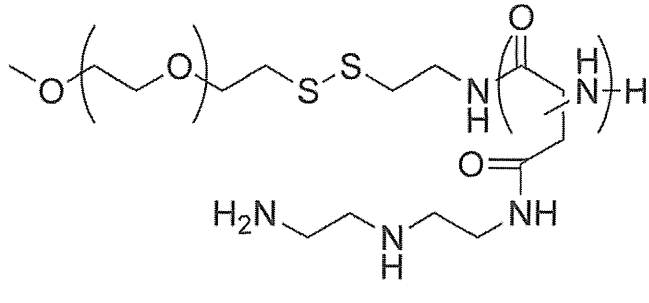

Fig. 1. Chemical structure of PEG-SS-PAsp(DET).

2.5. Dynamic light scattering (DLS) and ζ-potential measurements

DLS and ζ-potential measurements were carried out at 25 °C using an ELSZ-SV2 (Otsuka Electronics Co., Ltd., Osaka, Japan), equipped with a He–Ne ion laser (633 nm) as the incident beam. The polyplex solutions were prepared at 250 μg pDNA/mL in 10 mM Tris–HCl buffer (pH 7.4) at N/P ratio = 10. In the DLS mesurement, the light scattering data were obtained with a detection angle of 160° at 25 °C. The rate of decay in the photon correlation function was analyzed by the cumulant method, and the corresponding hydrodynamic diameter of the polyplexes was then calculated by the Stokes–Einstein equation. In the case of ζ-potential measurement, the ζ-potential was calculated from the obtained electrophoretic mobility by the Smoluchowski equation:

$$\zeta = 4\pi\eta\upsilon/\varepsilon$$

where η is the viscosity of the solvent, υ is the electrophoretic mobility, and ε is the dielectric constant of the solvent.

2.6. Cell lines

Human pancreatic carcinoma SUIT-2 was obtained from the American Type Culture Collection. SUIT-2 stably expressing luciferase protein (SUIT-2/luc) was established by cloning with limiting dilution method after transfecting a multiply attenuated lenti viral vector for luciferase gene provided by Dr. Takafumi Nakamura (The University of Tokyo). SUIT-2 and SUIT-2/luc cells were grown in RPMI1640 (Wako Pure Chemical Industries, Ltd.) supplemented with 10% heat-inactivated fetal bovine serum (FBS, Wako Pure Chemical Industries, Ltd.), 100 U/mL penicillin and 100 μg/mL streptomycin at 37 °C in humidified air containing 5% CO_2.

2.7. Animals

BALB/c nude and BALB/c mice (female, 6 weeks old) were purchased from Charles River Laboratories (Tokyo, Japan). Animals were housed in a temperature-controlled room under 12:12 h light:dark cycles and allowed to access food and water *ad libitum*. Experiments were carried out in compliance with the Guidelines for Animal Experiments of the Kyushu University, and approved by the Animal Care and Use Committee of Kyushu University.

2.8. Kinetic assay for transgene expression by in vivo bioluminescent imaging

BALB/c nude mice were intraperitoneally inoculated with SUIT-2 cells (1×10^6 cells/mouse). One week later, polyplex micelles consisting of 100 μg of pCpG-ΔLuc and block copolymers were administered intraperitoneally. *In vivo* bioluminescent imaging (BLI) was performed with an IVIS Imaging System (Xenogen Biosciences, Alameda, CA) and the bioluminescent signals were analyzed using Living Image software (Xenogen Biosciences, Alameda, CA). At 20 min prior to *in vivo* imaging, animals received the substrate D-Luciferin (Summit Pharmaceuticals International Corporation, Tokyo, Japan) at 75 mg/kg in 10 mM phosphate buffered solution (pH = 7.4) by intraperitoneal injection under anesthesia with the inhalation of 3% isoflurane (Abbot Laboratories, North Chicago, IL).

2.9. Antitumor activity of RGD4C-hTNF-α gene therapy for peritoneal dissemination

BALB/c nude mice (female, n = 10 in each group) were intraperitoneally inoculated with SUIT-2/luc cells (2×10^5 cells/mouse). Tumors were allowed to grow for 1 week. Subsequently, polyplex micelles of PEG-SS-P[Asp(DET)] or PEG-P[Asp(DET)] (50 μg of pVIVO-RGD4C-hTNF-α; N/P ratio = 10) or saline were administered into the peritoneal cavity of mice. We used pVIVO-RGD4C-hTNF-α for cancer therapy experiments, because the GRP promoter of pVIVO1 yields persistently higher expression within the tumor microenvironments than elongation factor-1 promoter of pCpGfree mcs plasmid. In a separate experiment, we confirmed the antitumor efficacy of RGD4C-hTNF-α by comparing pCpG-RGD4C-hTNF-α and mock (pCpGfree-mcs) plasmids to delete immunogenic CpG motifs in peritoneal dissemination model (Supplementary Fig. 1). *In vivo* bioluminescent imaging (BLI) was performed with an IVIS Imaging System as described above (Section 2.8). The survival of the mice was evaluated in each group up to 120 days after the inoculation.

2.10. Analysis of RGD4C-hTNF-α expression by quantitative real-time reverse-transcriptional PCR (qRT-PCR)

The expression of RGD4C-hTNF-α mRNA in tumor and normal organ tissues was evaluated by qRT-PCR. At 24 h after the injection of polyplex micelles, tumor and the other organ tissues (spleen, liver, kidney, lung and intestine) were obtained and snap-frozen in liquid nitrogen for the following assays. Total RNA was extracted using illustra™ RNAspin Mini RNA Isolation Kit (GE Healthcare UK, Ltd., Buckinghamshire, UK) according to the manufacturer's instruction, and subjected to cDNA synthesis using Transcriptor First Strand cDNA synthesis Kit (Roche Applied Science, Mannheim, Germany). Quantitative real-time PCR for RGD4C-hTNF-α and β-actin as a housekeeping gene was performed using hTNF-α primers: 5′-CAGCCTCTTCTCCTTCCTGAT-3′ and 5′-GCCAGAGGGCTGATTAGAGA-3′; β-actin primers and Universal Probe library set (Roche Applied Science) in the LightCycler480 II system (Roche Diagnostics, Mannheim, Germany).

2.11. Immunohistochemical analysis of RGD4C-hTNF-α expression

Tissue samples obtained on day 1 after injection of polyplex micelles were embedded in OCT compounds and frozen in cold acetone. Frozen sections (8–10 μm) were air dried and fixed in cold acetone for 10 min. After blocking with 3% bovine serum albumin (BSA), the sections were incubated with a rat anti-human TNF-α antibody (1:250; MCA1560, AbD Serotec, Kidlington, UK) at room temperature for 1 h, followed by a biotinylated rabbit anti-rat IgG(H + L) (1:250; BA-4001, Vector Laboratories Inc., Burlingame, CA) for 10 min. The sections were stained with horseradish peroxidase-conjugated streptavidin (PK-6100, Vector Laboratories Inc.) and 3,3′-diaminobenzidine (DAB) substrate kit (SK-4100, Vector Laboratories Inc.).

2.12. Histochemical analysis for the in vivo distribution of polyplex micelle

Fluolid Orange NHS (International Science Technology Co. LTD., Fukuoka, Japan) was conjugated to amino groups of polycations, such as PEG-P[Asp(DET)] and PEG-SS-P[Asp(DET)], according to the manufacturer's protocol. Fluolid Orange-labeled polyplex micelles loading pDNA were intraperitoneally injected at a dose of 50 μg/mouse. Mice were sacrificed after 24 h and excised organs were frozen in OCT compounds. The frozen samples were further sectioned at a 10-μm thickness in a cryostat. The nuclei were stained with DAPI. The samples were observed by confocal scanning laser microscopy NIKON A1 (NIKON CORPORATION, Tokyo, Japan).

2.13. Hepatic and renal function tests

Polyplex micelles consisting of pVIVO-RGD4C-hTNF-α (50 μg/mouse, N/P ratio = 10) were intraperitoneally administered to BALB/c mice (female, n = 6). Blood was collected from the vena cava at 4, 24, and 72 h, allowed to coagulate for 4 h at 4 °C and then serum was isolated as the supernatant fraction following centrifugation at 2000 *g* for 10 min.

To assess hepatic and renal toxicities of polyplex micelles, serum concentrations of alanine aminotransferase (ALT) and creatinine were determined by Japan Society of Clinical Chemistry (JSCC) transferable and enzyme methods, respectively, with 7180 Clinical Analyzer (Hitachi, Tokyo, Japan). Body weight changes were monitored as an index of overload influence for whole body.

2.14. Statistical analysis

Results are represented as means ± standard deviation (SD). Data were statistically analyzed using Student's *t*-test. Survival was analyzed by Kaplan–Meier method with a log-lank test. A P value less than 0.05 was considered to represent a statistically significant difference.

3. Results

3.1. Polyplex micelle characterization

As shown in Table 1, the polyplexes from PEG-SS-P[Asp(DET)] and PEG-P[Asp(DET)] formed the micelles in equivalent diameter at the range of 80–90 nm. The polyplex micelles from the block copolymer showed almost neutral ζ-potential values (~2 mV) due to the shielding by a PEG palisade surrounding the polyplex core.

3.2. Kinetics assay for luciferase activity by bioluminescence imaging in vivo

Fig. 2 shows the time-course changes in luciferase activity *in vivo* after intraperitoneal injection of polyplex micelles with the reporter gene. The luciferase activity was elevated with the peak at 24 h after injection ($P<0.05$, each polyplex micelle-treated *versus* control group). The activities were gradually declined, but sustained more than 4.2 and 2.7×10^5 photons/s for PEG-SS-P[Asp(DET)] and PEG-P[Asp(DET)] groups, respectively, on day 7, which were higher ($P<0.05$) than the control ($1.2\pm0.4\times10^5$ photons/s). Next, we compared the level of transgene expression between polyplex micelles. PEG-SS-P[Asp(DET)] exhibited 2-orders of magnitude higher luciferase activity ($1.8\pm1.6\times10^8$ photons/s) than PEG-P[Asp(DET)] ($3.0\pm1.4\times10^6$ photons/s, $P<0.05$) on day 1 after polyplex micelle injection. The luciferase activity was still higher in PEG-SS-P[Asp(DET)] than PEG-P[Asp(DET)] group on days 2 and 4 ($P<0.05$). On day 7 after injection, there was no significant difference between the two groups.

3.3. Transgene expression in tumor and normal organ tissues

Expression levels of therapeutic gene: RGD4C-hTNF-α were evaluated by the qRT-PCR in various tissues (Fig. 3). PEG-SS-P[Asp(DET)] and PEG-P[Asp(DET)] polyplex micelles induced 100-fold higher expression of RGD4C-hTNF-α in tumor nodules compared to the control ($P<0.05$, Fig. 3B). Similarly, each polyplex group showed significantly higher RGD4C-hTNF-α expressions compared to control in some tissues, such as spleen and liver ($P<0.05$, Fig. 3C,D). Other tissues of kidney, lung and intestine showed faint transgene expression (Fig. 3E,F,G).

Next, we compared RGD4C-hTNF-α expression levels between each polyplex micelle. PEG-SS-P[Asp(DET)] polyplex micelles-treatment resulted in 5.0-fold higher ($P=0.028$) expressions of RGD4C-hTNF-α than those of PEG-P[Asp(DET)] in tumor. In spleen and liver, there was no significant difference in RGD4C-hTNF-α expression between PEG-SS-P[Asp(DET)] and PEG-P[Asp(DET)] polyplex micelles.

The expression of RGD4C-hTNF-α protein was also confirmed by immunohistochemical analysis in tumor nodules after administration of the PEG-SS-P[Asp(DET)] and PEG-P[Asp(DET)] polyplex micelles (Fig. 4A). The transduced RGD4C-hTNF-α was detected in tumor tissues, and the localization was predominately detected in peripheral tumor sites. The expression of RGD4C-hTNF-α was also observed in spleen and lymph nodes for PEG-SS-P[Asp(DET)] and PEG-P[Asp(DET)]

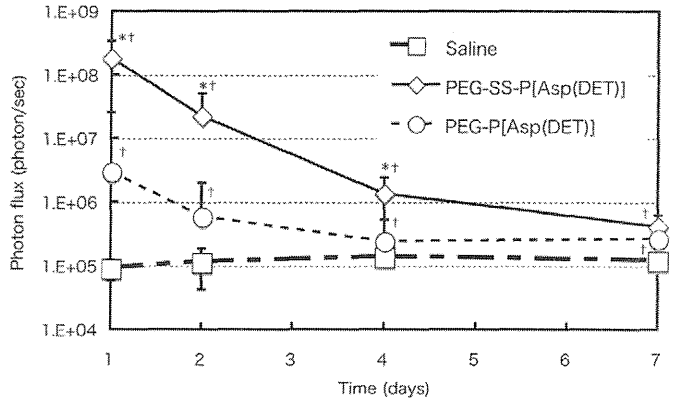

Fig. 2. Luciferase activities after intraperitoneal administration of two types of polyplex micelles loaded with a luciferase gene or saline. The time-dependent changes in luciferase activities were evaluated with an IVIS Imaging System. Saline (□); PEG-SS-P[Asp(DET)](◇); PEG-P[Asp(DET)] (○) (n=6 in each group; * $P<0.05$ *versus* PEG-P[Asp(DET)]; † $P<0.05$ *versus* saline).

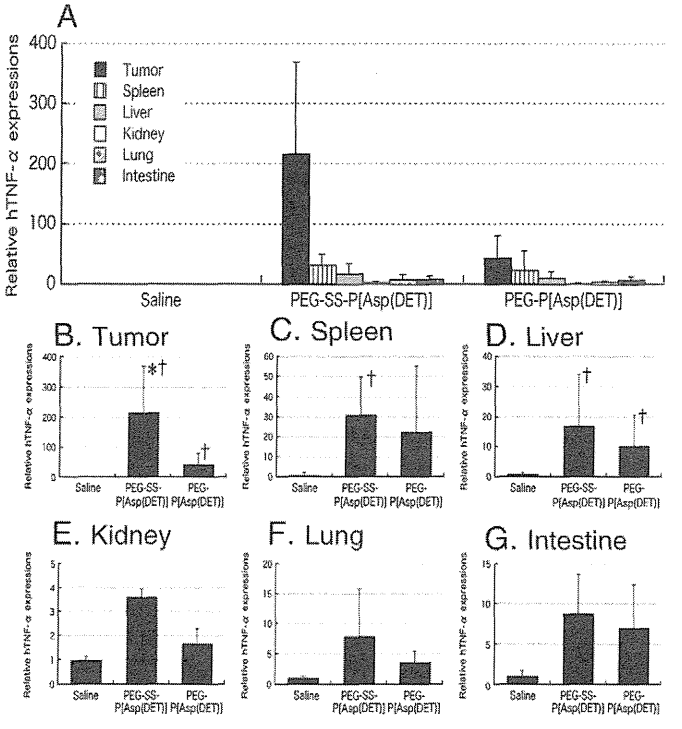

Fig. 3. Evaluation of RGD4C-TNF-α gene expression in organs by qRT-PCR. Saline and two types of polyplex micelles (50 μg pDNA/mouse) were i.p. injected into mice bearing SUIT-2 disseminated cancers. On day 1 after injection, the organ tissues were excised, and the total RNA were extracted and subjected to the quantification of RGD4C-TNF-α expression by qRT-PCR (A). The below graphs represent for tumor (B), spleen (C), liver (D), kidney (E), lung (F) and intestine tissues (G). Results are means ± standard deviations (n=3 in each group; * $P<0.05$ *versus* PEG-P[Asp(DET)]; † $P<0.05$ *versus* saline).

Table 1
Particle size and ζ-potential of polyplex micelles.

	Size (nm)	ζ-potential (mV)
PEG-SS-P[Asp(DET)]	84.7 ± 0.60	1.97 ± 1.16
PEG-P[Asp(DET)]	86.1 ± 0.48	1.55 ± 0.41

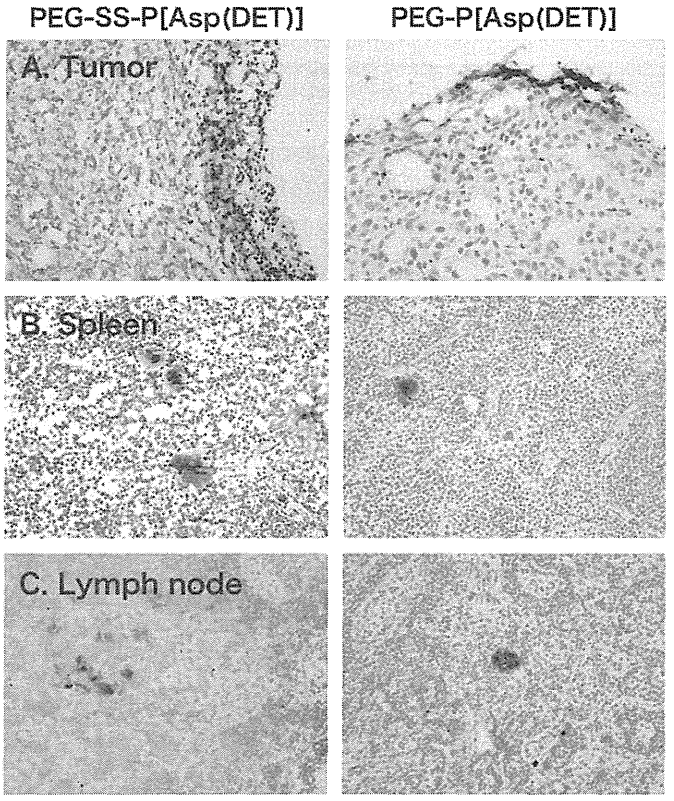

Fig. 4. Immunostaining of RGD4C-hTNF-α in (A) tumor (×10), (B) spleen (×10) and (C) lymph nodes (×20). The polyplex micelles (50 μg pVIVO-RGD4C-hTNF-α pDNA/mouse) were i.p. injected into mice bearing SUIT-2 disseminated cancers. On day 1 after injection, the organs were excised and immunostained with a primary anti-human TNF-α antibody, followed by a secondary anti-rat IgG and a subsequent DAB substrate.

groups (Fig. 4B,C). The RGD4C-hTNF-α signals were located not only in subserous area but also in white pulp of spleen area.

3.4. In vivo distribution of polyplex micelles

The delivered locus of polyplex micelle was analyzed by confocal laser microscopic detection of Fluolid Orange labeled polycation (Fig. 5) in various tissues. There was no significant difference in tissue distribution between PEG-SS-P[Asp(DET)] and PEG-P[Asp(DET)] polyplex micelles. The two types of polyplex micelles were mainly found in stromal regions of tumor tissues at 24 h after i.p. administration (Fig. 5A). Fluolid signals were also detected in the white pulp of the spleen and lymph nodes post administration of PEG-SS-P[Asp(DET)] polyplex micelles as similarly as PEG-P[Asp(DET)] (Fig. 5B). In the liver, Fluolid signals were sparsely observed in hepatic parenchymal area for either polyplex micelle group (Fig. 5C). The kidney, lung, intestine, brain, ovary and heart were not detected for Fluolid signals either in PEG-SS-P[Asp(DET)] or PEG-P[Asp(DET)] groups (data not shown).

3.5. Antitumor activity

To compare the antitumor effect of the polyplex micelles encapsulated with RGD4C-hTNF-α gene, we evaluated the disseminated tumor volume by bioluminescent signals from luciferase-transfectant pancreatic cancers. The changes in relative tumor volume (V/V_0) after single i.p. administration of polyplex micelles are shown in Fig. 6A. The time-dependent increases in tumor volume were observed in the saline-control group (4.7 ± 4.1 on day 7; 48.9 ± 40.3 on day 14; 65.2 ± 63.6 on day 21). The tumor growth was also found in PEG-P[Asp(DET)] group (2.6 ± 1.5 on day 7; 8.0 ± 4.8 on day 14; 44.0 ± 42.2 on day 21), although the growth speed was decreased by PEG-P[Asp(DET)] polyplex micelles-treatment ($P<0.05$). On the other hand, the growth suppression was obviously induced by PEG-SS-P[Asp(DET)] polyplex micelles-treatment (2.2 ± 2.0 on day 7; 2.7 ± 2.3 on day 14; 5.2 ± 2.1 on day 21). There were significant differences in tumor growth between PEG-SS-P[Asp(DET)] group ($P<0.05$), PEG-P[Asp(DET)] and control groups.

We next compared the survival between the polyplex micelles-treated and control mice. The median survival of the PEG-P[Asp(DET)] group was longer than that of control mice (57.3 ± 7.9 *versus* 43.5 ± 7.5 days, $P<0.05$) (Fig. 6B). The survival of the PEG-SS-P[Asp(DET)] group (65.9 ± 6.8 days) was further prolonged ($P<0.05$) than those of PEG-P[Asp(DET)] and control groups.

3.6. Toxicity study of polyplex micelles

The serum ALT concentrations as an index of hepatic toxicity did not increase during the observation time in all groups. There were no differences in ALT between the polyplex micelles-treated, saline and untreated mice (Table 2A). The creatinine concentrations as an index of renal toxicity also did not change, and no significance was observed between the two polyplex group, saline and untreated mice (Table 2B). Body weight was monitored as an indicator of overload influence for whole body. It is clear that each group has no observable side effects at 50 μg pDNA dosage except PEG-SS-P[Asp(DET)] group at 24 h after i.p. administration in this study (Fig. 7).

4. Discussion

A challenging demand in the field of non-viral gene therapy is to provide efficient transduction without significant toxicity. In the present study, we explored the biodistribution, gene expression, therapeutic efficacy and safety potentials of PEG-detachable polyplex micelle as a gene carrier *in vivo* to verify our hypothesis that the PEG release from polycation contributes to the increase in transduction efficiency without toxicity.

PEG-SS-P[Asp(DET)] exhibited higher level of RGD4C-hTNF-α gene expression in tumor tissue than that of PEG-P[Asp(DET)] by qRT-PCR analysis (Fig. 3B). It should be noted that PEG-SS-P[Asp(DET)] reveals almost 2 order of magnitude higher *in vitro* [22] and *in vivo* kinetics study for reporter gene expression than PEG-P[Asp(DET)] (Fig. 2). On the other hand, the distributed location and amount of PEG-SS-P[Asp(DET)] and PEG-P[Asp(DET)] polyplex micelles did not differ remarkably based on the data of Fluolid histochemical analysis (Fig. 5A). These results suggest that the major cause for high transgene expression in tumor with the polyplex micelles from the PEG-SS-P[Asp(DET)] may be not the difference in distributed amount of micelles into tumors. A previous study [22] has reported that confocal laser scanning microscopy shows the facilitated endosomal escape of pDNA with the PEG-SS-P[Asp(DET)] but not much with PEG-P[Asp(DET)] in culture cells. Although the intracellular trafficking of Fluolid in tissues was practically difficult (data not shown), PEG detachment may lead to facilitated transfection in the intracellular stage.

Considering the mechanism of tumor-targetability of polyplex micelles, biodistribution of polyplex micelles should be addressed to several aspects of enhanced permeability and retention (EPR) effect [32] and direct penetration into tumor tissues. Possible route of gene transfer is a direct infiltration of polyplexes to tumor tissues through its surface. The organs in the peritoneal cavity are normally covered with the peritoneum, subperitoneal connective tissue and serosa, whereas the disseminated tumor nodules are devoid of such coverings, since the interaction of cancer cells with the peritoneum induces disruption and exfoliation of the mesothelial cells in the early process of peritoneal metastasis [33,34]. Tumor tissues without such

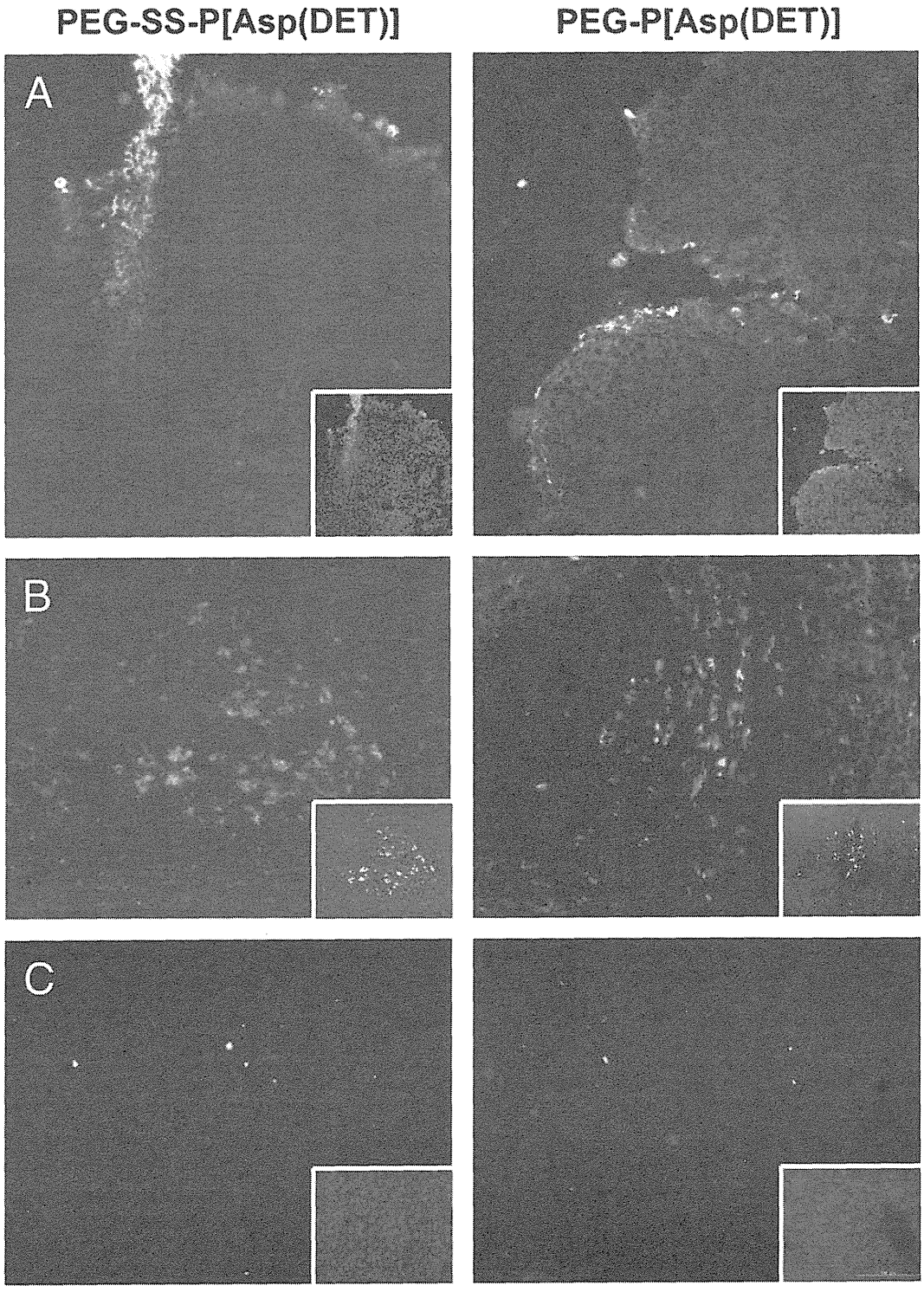

Fig. 5. Polyplex micelle localization in tumor (A), spleen (B) and liver (C). Fluolid Orange-signals labeled polyplex micelles (orange) were detected in tumor and normal organ tissues by laser confocal microscopy at 24 h after polyplex micelle administration. The cell nuclei were stained with DAPI (blue).

barriers could be infiltrated with the polyplexes. Another possible route of gene transfer is a tumor accumulation *via* blood vessels by EPR effect [32]. However, the proportion in tumor accumulation of polyplexes *via* blood vessels might not be dominant, since large molecular compounds (M.W. > 20, 000) do not efficiently drain from peritoneal cavity to blood vessels [35,36]. An additional element which may account for the tumor-preference is that the transduced gene is more readily expressed in proliferating cells, such as cancer and inflammatory cells, but little in normal quincent cells [37]. Fig. 3 showed that there are no significant differences in transgene expressions in normal organs between the two types of micelles. The disulfide linkage might be cleaved more effectively in tumor tissues, because tumors are under more reducing conditions compared to normal organs [38]. Since transfected gene is transported to the nucleus inefficiently

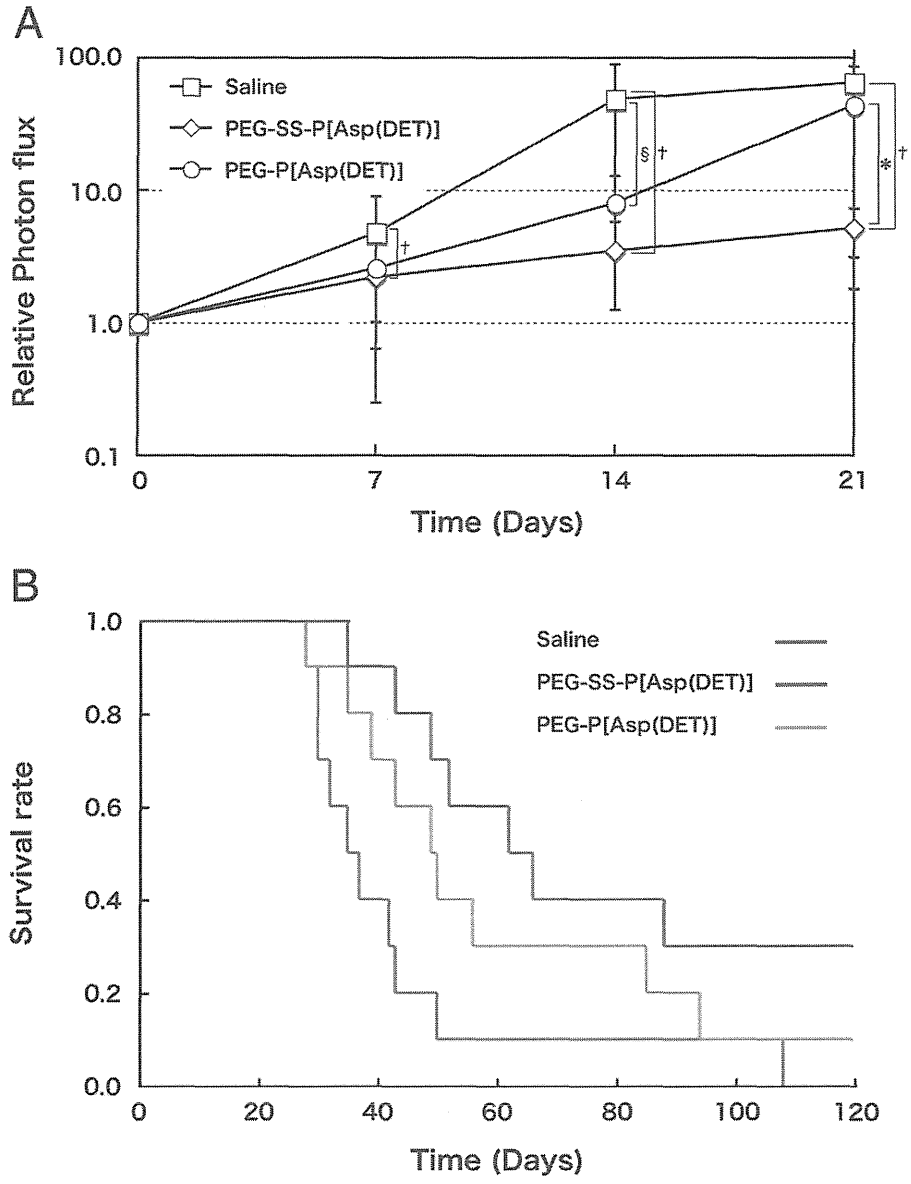

Fig. 6. Antitumor activity of polyplex micelles with pVIVO-RGD4C-hTNF-α pDNA in mice with SUIT-2/luc peritoneal dissemination. (A) Relative photon flux evaluated by IVIS imaging system for intraperitoneal metastatic sites of SUIT-2/luc in mice treated with polyplex micelles. Saline (□); PEG-SS-P[Asp(DET)](◇); PEG-P[Asp(DET)] (○). Data are expressed as averages ± standard deviations (* $P<0.05$ *versus* PEG-P[Asp(DET)]; † $P<0.05$ *versus* saline). (B) Kaplan–Meier analysis for survival of mice bearing peritoneal dissemination that received i.p. injection of saline, PEG-SS-P[Asp(DET)] or PEG-P[Asp(DET)] polyplex micelles.

through the nuclear membrane during interphase, it is likely that the breakdown of the nuclear membrane during cell cycle may be crucial for efficient transgene expression [39,40].

An interesting finding in our fluorescence study is that i.p. administered polyplexes tended to be predominantly delivered into stromal regions of peripheral tumor tissues (Fig. 5A). PEG-SS-P[Asp(DET)] and PEG-P[Asp(DET)] polyplex micelles accumulated in stromal regions but not inside the tumor nests, because high tumor cell density is a barrier of polyplex micelle infiltration. Drug penetration is impeded by severe fibrosis and high interstitial pressure [41–43]. These physiobiological features of tumor nodules are thought to be involved in the unique distribution of polyplex micelles after i.p. injection.

PEG-SS-P[Asp(DET)] and PEG-P[Asp(DET)] polyplex micelles also transduced gene expression in spleen and liver (Fig. 3C, D), while the degree of gene expression and distribution to spleen and liver was similar in both polyplex micelles (Fig. 5B, C). Expression loci were mainly in the inner area, but not in the outer layer area, of the spleen, liver and lymph nodules (Fig. 4B, C). The transgene expression profile in various organs after i.p. injection of the polyplexes is different from that after intravenous injection, in which the lung, liver and kidney appear as preferential expression sites, probably as a consequence of the filtration function of these organs [44–48]. The polyplexes after i.p. injection might enter into the lymphatics and portal blood vessels predominantly and consequently distribute the lymphatic and liver tissue, but minorly into systemic blood circulation to distant organs, such as lung and kidney. Large molecular compounds (M.W.>20,000) hardly penetrate into normal tissues, whereas they drain to lymphatic systems regardless of size and charge of nanoparticles [35,36]. This property of distribution with lymphatic tropism indicates that the strategy of i.p. administration would be effective to activate immunity in the lymphatic tissues, leading to the application for immuno-gene therapy.

In peritoneal disseminated cancer model, PEG-SS-P[Asp(DET)] polyplex micelles encapsulating pVIVO-RGD4C-hTNF-α plasmid inhibited the proliferation of tumors more effectively compared

Table 2
Evaluation of hepatic and renal toxicity after intraperitoneal administration of two types of polyplex micelles encapsulating pVIVO-RGD4C-hTNF-α. Serum ALT (A) and creatinine (B) levels were measured at 4, 24, and 72 h after i.p. administration of polyplex micelles in mice (n = 6 in each group).

Time (h)	Normal	Saline	PEG-SS-P[Asp(DET)]	PEG-P[Asp(DET)]
(A) ALT				
4	44.6 ± 21.5	53.7 ± 18.0	45.8 ± 21.9	48.0 ± 20.4
24		64.0 ± 31.5	68.0 ± 14.6	56.5 ± 16.1
72		56.0 ± 17.4	48.6 ± 7.8	48.0 ± 9.3
(B) Creatinine				
4	0.14 ± 0.03	0.15 ± 0.01	0.12 ± 0.02	0.13 ± 0.02
24		0.16 ± 0.02	0.16 ± 0.02	0.14 ± 0.03
72		0.15 ± 0.01	0.15 ± 0.02	0.12 ± 0.03

with PEG-P[Asp(DET)] polyplex micelles (Fig. 6A). In addition, PEG-SS-P[Asp(DET)] polyplex micelles significantly prolonged the survival for mice with peritoneal dissemination compared with PEG-P [Asp(DET)] polyplex micelles (Fig. 6B). The antitumor effects might be mediated by paracrine action of RGD4C-TNF-α to tumor and vascular endothelial cells from the polyplex micelles in tumor stroma, although subsets of tumor species gain the resistance to TNF-α [49]. The production level of RGD4C-hTNF-α production from PEG-SS-P [Asp(DET)] polyplex micelles was significantly higher than that from PEG-P[Asp(DET)] polyplex micelles (Fig. 3B). High-dose TNF-α causes destruction of newly formed blood vessels [50] and TNF-α induces a dose-dependent reduction of tumor blood flow [51,52]. TNF-α is also known to activate NK and macrophage cells, which might be partly responsible for the antitumor effect of RGD4C-hTNF-α gene therapy on peritoneal disseminated cancer. Furthermore, we constructed RGD4C-hTNF-α expression plasmid gene to increase the specificity of tumor vessels, because RGD4C peptide moiety specifically binds the integrin $\alpha_v\beta_3$, which is overexpressed on tumor vascular endothelial cells [29]. These evidences suggest that the higher local RGD4C-hTNF-α gene expression produced by PEG-SS-P[Asp(DET)] polyplex micelles eradicate tumor vasculature much more than PEG-P [Asp(DET)] polyplex micelles, resulting in an effective inhibition of the progression of disseminated tumor.

To evaluate the toxicity of polyplex micelles, we performed hepatic and renal function tests in mice at several time points after transduction with RGD4C-hTNF-α expression plasmid. A previous report [53] showed that systemically administered pDNA/cationic liposome complex induced toxicity in the liver mainly and not in the lung. In contrast, the hepatic function of mice treated with PEG-SS-P[Asp(DET)] and PEG-P[Asp(DET)] polyplex micelles encapsulating pVIVO-RGD4C-hTNF-α plasmid were kept normal as similarly as untreated mice (Table 2A). These results indicated that polyplex micelles are not toxic to liver tissues when the current dose was administered *via* i.p., although polyplex micelles were distributed to the liver (Fig. 5C). Secondly, no change in serum creatinine level suggests that PEG-SS-P[Asp(DET)] and PEG-P[Asp(DET)] polyplex micelles induce no nephrotoxicity (Table 2B). This could be explained by the low expression of RGD4C-hTNF-α gene in the kidney (Fig. 3E) due to little distribution of polyplex micelles to this organ (data not shown). This was consistent with the previous report for PEI [54]. Moreover, no significant body weight loss was observed after i.p. administration of polyplex micelles except the transient decrease at 24 h, when surgical and anesthesia stress together with polyplex i.p. irritation might limit the intake of water and food, despite hepatic and renal functions were intact. TNF-α fusion protein has effective antitumor effects by repeated administrations [29], and has been tried for clinical application as an antineoplastic agent [55,56]. However, clinical applications of TNF-α fusion protein for cancer therapy are still limited, because systemic administration of TNF-α protein induces toxic side effects [57,58], such as fever and decreased blood pressure, and the drug concentration at the tumor sites does not reach to the range of therapeutic dose due to the dilution factor after systemic administration [59], although recombinant TNF-α protein might be effective with minimal toxicity when infused by intraperitoneal administration, not by systemic administration. On the other hand, administration of PEG-detachable polyplex micelles encapsulating pVIVO-RGD4C-hTNF-α plasmid showed no remarkable toxic side effects, while the local expression of RGD4C-hTNF-α from the polyplex micelles in tumor stroma leads to sustain the concentration of this cytokine enough to exhibit the antitumor effect, even by single-administration regimen. In addition, TNF-α based gene therapy may have synergistic potential for tumor eradication when combined with ganciclovir suicide gene [60] and irradiation/chemotherapy [61] despite of investigational therapy to date. Our polymeric micelle systems can be also applied for cotransfection with same platform. These results suggest that i.p. administration of PEG-detachable polyplex micelles encapsulating pVIVO-RGD4C-hTNF-α plasmid may have advantages in wide capacity for safety in the diseased condition with peritoneal disseminated tumors.

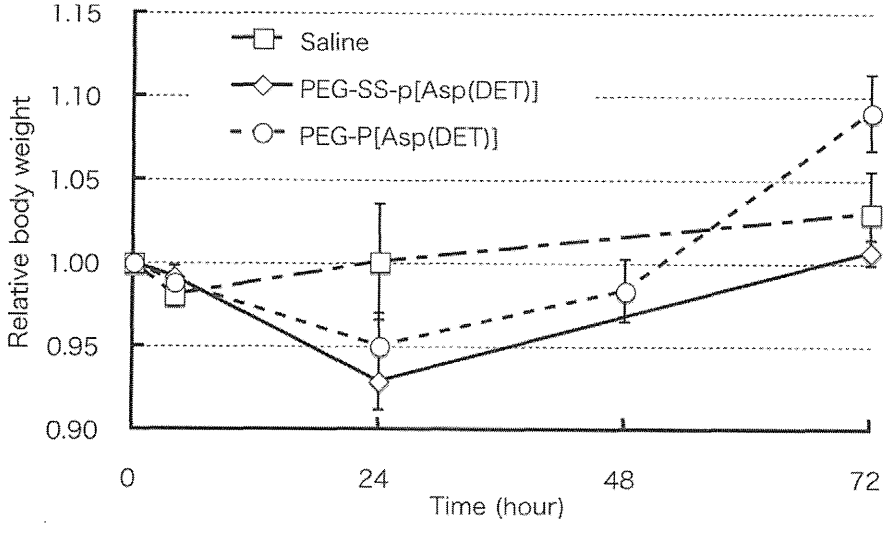

Fig. 7. Changes in body weight of mice treated with two types of polyplex micelles encapsulating pVIVO-RGD4C-hTNF-α. Saline (□); PEG-SS-P[Asp(DET)](◇); PEG-P[Asp(DET)] (○) (n = 6 in each group).

In conclusion, we have demonstrated that PEG-detachable polyplex micelles exhibit an appreciable transgene expression in tumor, spleen and liver without significant toxicity, resulting in the antitumor efficacy for peritoneally disseminated cancer. The safe and effective modality for peritoneal dissemination could be achieved by gene therapy using PEG-detachable polyplex micelles in future clinical applications.

Acknowledgments

This work was financially supported in part by the Grants-in-Aid for Scientific Research to K.N. from the Japanese Ministry of Education, Culture, Sports, Science and Technology, Japan (MEXT) (project code: 21390374). This research is also partly supported by the Funding Program for World-Leading Innovation R&D on Science and Technology (FIRST Program) from the Japan Society for the Promotion of Science (JSPS), initiated by the Council for Science and Technology Policy (CSTP), and the Core Research Program for Evolutional Science and Technology (CREST) from Japan Science and Technology Agency (JST). We appreciate Mrs. Michiko Fujita (The University of Tokyo), Mrs. Aya Sakai and Mr. Takaaki Kanemaru (Kyushu University) for technical assistance.

Appendix A. Supplementary data

Supplementary data to this article can be found online at doi:10.1016/j.jconrel.2012.03.021.

References

[1] M.A. Kay, State-of-the-art gene based therapies: the road ahead, Nat. Rev. Genet. 12 (5) (2011) 316–328.
[2] F. Mingozzi, K.A. High, Therapeutic *in vivo* gene transfer for genetic disease using AAV: progress and challenges, Nat. Rev. Genet. 12 (5) (2011) 341–355.
[3] D.W. Pack, A.S. Hoffman, S. Pun, P.S. Stayton, Design and development of polymers for gene delivery, Nat. Rev. Drug Discov. 4 (7) (2005) 581–593.
[4] T. Merdan, J. Kopecek, T. Kissel, Prospects for cationic polymers in gene and oligonucleotide therapy against cancer, Adv. Drug Deliv. Rev. 54 (2002) 715–758.
[5] M. Meyer, E. Wagner, Recent developments in the application of plasmid DNA-based vectors and small interfering RNA therapeutics for cancer, Hum. Gene Ther. 17 (11) (2006) 1062–1076.
[6] T.G. Park, J.H. Jeong, S.W. Kim, Current status of polymeric gene delivery systems, Adv. Drug Deliv. Rev. 58 (4) (2006) 467–486.
[7] K. Osada, R.J. Christie, K. Kataoka, Polyemric micelles from poly(ethylene glycol)-poly(amino acid) block copolymer for drug and gene delivery, J. R. Soc. Interface 6 (Suppl. 3) (2009) S325–S339.
[8] M. Neu, D. Fischer, T. Kissel, Recent advances in rational gene transfer vector design based on poly(ethylene imine) and its derivatives, J. Gene Med. 7 (8) (2005) 992–1009.
[9] S. Katayose, K. Kataoka, Water-soluble polyion complex associates of DNA and poly(ethylene glycol)-poly(L-lysine) block copolymer, Bioconjug. Chem. 8 (5) (1997) 702–707.
[10] S. Katayose, K. Kataoka, Remarkable increase in nuclease resistance of plasmid DNA through supramolecular assembly with poly(ethylene glycol)-poly(L-lysine) block copolymer, J. Pharm. Sci. 87 (2) (1998) 160–163.
[11] M. Ogris, S. Brunner, S. Schuller, S. Kircheis, E. Wagner, PEGylated DNA/transferring-PEI complexes: reduced interaction with blood components, extended circulation in blood and potential for systemic gene delivery, Gene Ther. 6 (4) (1999) 595–605.
[12] K.Y. Kwok, D.L. McKenzie, D.L. Evers, K.G. Rice, Formulation of highly soluble poly(ethylene glycol)-peptide DNA condensates, J. Pharm. Sci. 88 (10) (1999) 996–1003.
[13] K. Itaka, K. Yamauchi, A. Harada, K. Nakamura, H. Kawaguchi, K. Kataoka, Polyion complex micelles from plasmid DNA and poly(ethylene glycol)-poly(L-lysine) block copolymer as serum-tolerable polyplex system: physicochemical properties of micelles relevant to gene transfection efficiency, Biomaterials 24 (24) (2003) 4495–4506.
[14] K. Itaka, A. Harada, K. Nakamura, H. Kawaguchi, K. Kataoka, Evaluation by fluorescence energy transfer of the stability of nonviral gene delivery vectors under physiological conditions, Biomacromolecules 3 (4) (2002) 841–845.
[15] N. Kanayama, S. Fukushima, N. Nishiyama, K. Itaka, W.D. Jang, K. Miyata, Y. Yamasaki, U.I. Chung, K. Kataoka, A PEG-based biocompatible block catiomer with high buffering capacity for the construction of polyplex micelles showing efficient gene transfer toward primary cells, ChemMedChem 1 (4) (2006) 439–444.
[16] D. Akagi, M. Oba, H. Koyama, N. Nishiyama, S. Fukushima, T. Miyata, H. Nagawa, K. Kataoka, Biocompatible micellar nanovectors achieve efficient gene transfer to vascular lesions without cytotoxicity and thrombus formation, Gene Ther. 14 (13) (2007) 1029–1038.
[17] K. Itaka, S. Ohba, K. Miyata, H. Kawaguchi, K. Nakamura, T. Takato, U.I. Chung, K. Kataoka, Bone regeneration by regulated *in vivo* gene transfer using biocompatible polyplex nanomicelles, Mol. Ther. 15 (9) (2007) 1655–1662.
[18] M. Han, Y. Bae, N. Nishiyama, K. Miyata, M. Oba, K. Kataoka, Transfection study using multicellular tumor spheroids for screening non-viral polymeric gene vectors with low cytotoxicity and high transfection efficiencies, J. Control. Release 121 (1–2) (2007) 38–48.
[19] B. Brissault, A. Kichler, C. Leborgne, O. Danos, H. Cheradame, J. Gau, L. Auvray, C. Guis, Synthesis, characterization, and gene transfer application of poly(ethylene glycol-b-ethyleneimine) with high molar mass polyamine block, Biomacromolecules 7 (10) (2006) 2863–2870.
[20] M. Kursa, G.F. Walker, V. Roessler, M. Ogris, W. Roedl, R. Kircheis, E. Wagner, Novel shielded transferring-polyethylene glycol-polyethyleneimin/DNA complexes for systemic tumor-targeted gene transfer, Bioconjug. Chem. 14 (1) (2003) 222–231.
[21] K. Sagara, S.W. Kim, A new synthesis of galactose-poly(ethylene glycol)-polyethyleneimine for gene delivery to hepatocytes, J. Control. Release 79 (1–3) (2002) 271–281.
[22] S. Takae, K. Miyata, M. Oba, T. Ishii, N. Nishiyama, K. Itaka, Y. Yamasaki, H. Koyama, K. Kataoka, PEG-detachable polyplex micelles on disulfide-linked block catiomers as bioresponsive nonviral gene vectors, J. Am. Chem. Soc. 130 (18) (2008) 6001–6009.
[23] C. Brigand, C. Arvieux, F.N. Gilly, O. Glehen, Treatment of peritoneal carcinomatosis in gastric cancers, Dig. Dis. 22 (4) (2004) 366–373.
[24] E.D. Tetzlaff, P. Cen, J.A. Ajani, Emerging drugs in the treatment of advanced gastric cancer, Expert Opin. Emerg. Drugs 13 (1) (2008) 135–144.
[25] P. Jacquet, P.H. Sugarbaker, Peritoneal-plasma barrier, Cancer Treat. Res. 82 (1996) 53–63.
[26] T. Kamei, J. Kitayama, H. Yamaguchi, D. Soma, S. Emoto, T. Konno, K. Ishihara, H. Ishigami, S. Kaisaki, H. Nagawa, Spatial distribution of intraperitoneally administered paclitaxel nanoparticles solubilized with poly(2-methacryloxyethyl phosphorylcholine-co-n-butyl methacrylate) in peritoneal metastatic nodules, Cancer Sci. 102 (1) (2011) 200–205.
[27] S. Mocellin, C.R. Rossi, P. Pilati, D. Nitti, Tumor necrosis factor, cancer and anticancer therapy, Cytokine Growth Factor Rev. 16 (1) (2005) 35–53.
[28] H. Wang, Z. Yan, J. Shi, W. Han, Y. Zhang, Expression, purification, and characterization of a neovasculature targeted rmfTNF-α in *Escherichia coli*, Protein Expr. Purif. 45 (1) (2006) 60–65.
[29] H. Wang, K. Chen, W. Cai, Z. Li, L. He, A. Kashefi, X. Chen, Integrin-targeted imaging and therapy with RGD4C-TNF fusion protein, Mol. Cancer Ther. 7 (5) (2008) 1044–1053.
[30] Y. Akiyama, H. Otsuka, Y. Nagasaki, M. Kato, K. Kataoka, Selective synthesis of heterobifunctional poly(ethylene glycol) derivatives containing both mercapto and acetal terminals, Bioconjug. Chem. 11 (6) (2000) 947–950.
[31] M. Mitsui, M. Nishikawa, L. Zang, M. Ando, K. Hattori, Y. Takahashi, Y. Watanabe, Y. Takakura, Effect of the content of unmethylated CpG dunucleotides in plasmid DNA on the sustainability of transgene expression, J. Gene Med. 11 (5) (2009) 435–443.
[32] Y. Matsumura, H. Maeda, A new concept for macromolecular therapeutics in cancer chemotherapy: mechanism of tumoritropic accumulation of proteins and the antitumor agent smancs, Cancer Res. 46 (12) (1986) 6387–6392.
[33] Y. Kiyasu, S. Kaneshima, S. Koga, Morphogenesis of peritoneal metastasis in human gastric cancer, Cancer Res. 41 (3) (1981) 1236–1239.
[34] M.J. Niedbala, K. Crickard, R.J. Bernacki, Interaction of human ovarian tumor cells with human mesothelial cells grown on extracellular matrix. An *in vitro* model system for studying tumor cell adhesion and invasion, Exp. Cell Res. 160 (2) (1985) 499–513.
[35] K. Hirano, C.A. Hunt, Lymphatic transport of liposome-encapsulated agents: effects of liposome size following intraperitoneal administration, J. Pharm. Sci. 74 (9) (1985) 915–921.
[36] K. Hirano, C.A. Hunt, A. Strubbe, R.D. MacGregor, Lymphatic transport of liposome-encapsulated drugs following intraperitoneal administration — effect of lipid composition, Pharm. Res. 6 (1985) 271–278.
[37] A. Kikuchi, Y. Aoki, S. Sugaya, T. Serikawa, K. Takakuwa, K. Tanaka, N. Suzuki, H. Kikuchi, Development of novel cationic liposomes for efficient gene transfer into peritoneal disseminated tumor, Hum. Gene Ther. 10 (6) (1999) 947–955.
[38] G.K. Balendiran, R. Dabur, D. Fraser, The role of glutathione in cancer, Cell Biochem. Funct. 22 (6) (2004) 343–352.
[39] F. Labat-Moleur, A.M. Steffan, C. Brisson, H. Perron, O. Feugeas, P. Furstenberger, F. Oberling, E. Brambilla, J.P. Behr, An electron microscopy study into the mechanism of gene transfer with lipopolyamines, Gene Ther. 3 (11) (1996) 1010–1017.
[40] M. Wilke, E. Fortunati, M. van den Broek, A.T. Hoogeveen, B.J. Scholte, Efficacy of a peptide-based gene delivery system depends on mitotic activity, Gene Ther. 3 (12) (1996) 1133–1142.
[41] A.I. Minchinton, I.F. Tannock, Drug penetration in solid tumors, Nat. Rev. Cancer 6 (8) (2006) 583–592.
[42] M. Yashiro, Y.S. Chung, S. Nishimura, T. Inoue, M. Soma, Fibrosis in the peritoneum induced by scirrhous gastric cancer cells may act as "soil" for peritoneal dissemination, Cancer 77 (8 Suppl.) (1996) 1668–1675.
[43] R.K. Jain, Barriers to drug delivery in solid tumor, Sci. Am. 271 (1) (1994) 58–65.
[44] J.L. Coll, P. Chollet, E. Brambilla, D. Desplanques, J.P. Behr, M. Favrot, *In vivo* delivery to tumors of DNA complexed with linear polyethylenimine, Hum. Gene Ther. 10 (10) (1999) 1659–1666.
[45] D. Goula, C. Benoist, S. Mantero, G. Merlo, G. Levi, B.A. Demeneix, Polyethylenimine-based intravenous delivery of transgenes to mouse lung, Gene Ther. 5 (9) (1998) 1291–1295.
[46] A. Bragonzi, A. Boletta, A. Biffi, A. Muggia, G. Sersale, S.H. Cheng, C. Bordignon, B.M. Assael, M. Conese, Comparison between cationic polymers and lipids in mediating systemic gene delivery to the lungs, Gene Ther. 6 (12) (1999) 1995–2004.